



AMERICAN UNIVERSITY OF BEIRUT

NUMERICAL AND EXPERIMENTAL EFFECT OF HEATING  
AND COOLING CYCLES ON THE SKIN FRICTION OF  
ENERGY PILES IN SOFT CLAYS

by  
ABIR AHMAD AWAD

A thesis  
submitted in partial fulfillment of the requirements  
for the degree of Master of Engineering  
to the Department of Civil and Environmental Engineering  
of the Maroun Semaan Faculty of Engineering and Architecture  
at the American University of Beirut

Beirut, Lebanon  
May 2018

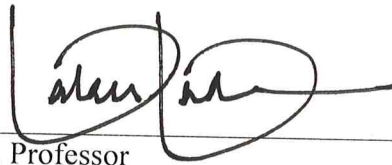
AMERICAN UNIVERSITY OF BEIRUT

NUMERICAL AND EXPERIMENTAL EFFECT OF HEATING AND  
COOLING CYCLES ON THE SKIN FRICTION OF ENERGY PILES  
IN SOFT CLAYS

by

ABIR AHMAD AWAD

Approved by:



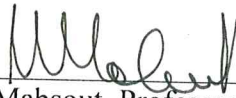
Dr. Salah Sadek, Professor  
Department of Civil and Environmental Engineering, AUB

Advisor



Dr. Shadi Najjar, Associate Professor  
Department of Civil and Environmental Engineering, AUB

Member of Committee



Dr. Mounir Mabsout, Professor  
Department of Civil and Environmental Engineering, AUB

Member of Committee

Date of thesis defense: May 3, 2018

AMERICAN UNIVERSITY OF BEIRUT

THESIS, DISSERTATION, PROJECT RELEASE FORM

Student Name: Awad Abir Ahmad

Last

First

Middle

Master's Thesis       Master's Project       Doctoral Dissertation

I authorize the American University of Beirut to: (a) reproduce hard or electronic copies of my thesis, dissertation, or project; (b) include such copies in the archives and digital repositories of the University; and (c) make freely available such copies to third parties for research or educational purposes.

I authorize the American University of Beirut, to: (a) reproduce hard or electronic copies of it; (b) include such copies in the archives and digital repositories of the University; and (c) make freely available such copies to third parties for research or educational purposes after:

**One ---- year from the date of submission of my thesis, dissertation, or project.**

**Two ---- years from the date of submission of my thesis, dissertation, or project.**

**Three ---- years from the date of submission of my thesis, dissertation, or project.**

  
Signature

May 15, 2018  
Date

## ACKNOWLEDGMENTS

It is a pleasure to thank the many people who made this thesis possible.

First and foremost, I offer my sincerest gratitude to my advisors Professor Salah Sadek and Professor Shadi Najjar. Without their assistance and dedicated involvement in every step throughout the process, this research would have never been accomplished. One simply could not wish for better or friendlier supervisors.

I would like to thank Professor Mounir Mabsout for being a committee member and providing the guidance and support. In addition, I would like to thank all staff and faculty members of the American University of Beirut for their assistance, especially the staff at the geotechnical laboratory.

Finally, I must express my very profound gratitude to my parents, fiancé and friends for providing me with unfailing support and continuous encouragement throughout the past two years and through the process of researching and thesis writing. This accomplishment would not have been possible without them. Thank you.

## AN ABSTRACT OF THE THESIS OF

Abir Ahmad Awad for

Master of Engineering

Major: Civil and Environmental Engineering

Title: Numerical and Experimental Effect of Heating and Cooling Cycles on the Skin Friction of Energy Piles in Soft Clays

Because of the current environmental problems, our planet is poised at the brink of a severe environmental crisis. This deviated the attention towards renewable energy, in particular, geothermal energy. In addition, with the increase of the use of deep foundation, integrating piles with geothermal systems became a trend. Although energy pile systems have been successfully used in the world, there are no clear design guides providing how thermal actions are considered in terms of safety and serviceability of energy piles (Bourne-Webb et al. 2016<sup>1</sup>). The primary function of energy piles is to safely carry loads while minimizing unacceptable movement or damage to the structure itself. A concern that arises from the use of structures with energy piles centers around the need to account for the possibility that the secondary use of the piles as heat exchangers could negatively affect the ability of the pile to carry the design load. The shear strength of the interface defines the stability of the pile and the thermo-hydro-mechanical changes, resulting from thermal cycles, affects the behavior of the interface at the saturated soil/ pile level. Published work on energy piles shows that in granular and very stiff, moderately to highly overconsolidated clayey soils, thermal effects on the mechanical properties of the soils may be neglected. However, heating may induce flow of water around the pile and could affect the skin friction and the adhesion between the pile and the surrounding soil. This issue has not been fully investigated in the literature. In this research, two small-scaled models were adopted to inspect this gap. These models aimed to study the effect of the thermal loading on the frictional capacity of the energy piles in saturated slightly overconsolidated clays with and without sustained static uplift load that is roughly 30% of the ultimate capacity. Results indicated that the ultimate capacity decreased compared to the control pile by observing a reduction in the adhesion factor in the order of 11 to 20 %, whereas, the vertical deformation of the geothermal piles due to sustained loading increased due to heating and cooling. These observations point to the importance of catering for geothermal effects on the serviceability and ultimate capacity of geothermal piles in normally to slightly over-consolidated clay.

# CONTENTS

ACKNOWLEDGEMENTS .....	v
ABSTRACT .....	vi
LIST OF ILLUSTRATIONS .....	x
LIST OF TABLES .....	xiii

Chapter	Page
1 INTRODUCTION .....	1
1.1 Introduction and Background .....	1
1.2 Literature Review .....	5
1.2.1 Energy Pile .....	5
1.2.2 Energy Pile: Types and Benefits .....	6
1.2.3 Thermal Response .....	7
1.2.3.1 Configurations .....	7
1.2.3.2 Soil and Fluids Characteristics .....	9
1.2.4 Experimental Research .....	10
1.2.5 Numerical .....	12
1.2.6 Design of Energy Piles .....	14
1.3 Thesis Objectives and Significance .....	15
1.3.1 Objective and Scope .....	15
1.3.1.1 Laboratory Experiments: .....	16
1.3.1.2 Coupled Simulations using PLAXIS .....	17
1.3.2 Significance .....	17
1.4 Thesis Organization .....	18
2 EXPERIMENTAL SETUP .....	19
2.1 Model Piles .....	19
2.2 Soils Tests .....	20
2.3 Soil Bed Preparation .....	25

2.4	Model Pile Installation .....	27
2.5	Instrumentation and Data Acquisition.....	29
3	EXPERIMENTAL MODEL I .....	30
3.1	Overview .....	30
3.2	Testing Procedure .....	30
3.2.1	Step 1 .....	30
3.2.2	Step 2 .....	31
3.2.3	Step 3 .....	32
3.2.4	Step 4 .....	32
3.3	Results .....	33
3.3.1	C-Pile .....	33
3.3.2	2U-Pile .....	33
3.3.3	S-Pile.....	36
3.3.4	Analysis.....	39
3.3.4.1	Thermal Cycles Results: .....	39
3.3.4.2	Uplift test results .....	41
4	EXPERIMENTAL MODEL II .....	44
4.1	Overview .....	44
4.2	Testing Procedure .....	45
4.2.1	Step 1 .....	45
4.2.2	Step 2 .....	45
4.2.3	Step 3 .....	46
4.3	Results .....	46
4.3.1	Working Load .....	46
4.3.2	Temperature results during cycles .....	46
4.3.2.1	2U-Pile cycles .....	46
4.3.2.2	S-Pile cycles .....	49
4.3.3	Head displacement and load results during cycles.....	52
4.3.4	Analysis.....	55
4.3.4.1	Thermal cycles results.....	55
4.3.4.2	Head Displacement .....	57
4.3.4.3	Uplift test results .....	59
5	RESULTS ANALYSIS.....	61



5.1	Thermal Response .....	61
5.2	Mechanical Response .....	64
5.3	Pile head displacement during cycles .....	65
6	FINITE ELEMENT MODEL .....	69
6.1	Model Parameters: .....	69
6.1.1	Geometry: .....	69
6.1.2	Material Characteristics: .....	70
6.2	Boundary Conditions: .....	71
6.2.1	Mechanical Boundary Conditions: .....	71
6.2.2	Thermal Boundary conditions: .....	71
6.3	Model Analysis .....	72
6.3.1	Mechanical Response .....	72
6.3.2	Thermal Response .....	74
7	CONCLUSION .....	78
	REFERENCES .....	80

## ILLUSTRATIONS

Figure	Page
1. Schematic view of a geothermal energy pile .....	6
2. Different heat tubing configurations .....	8
3. Model piles (a) S-Pile (b) C-Pile and (c) 2U-Pile.....	19
4. Configurations of the piles (a) 2U-Pile (b) C-Pile and (c) S-Pile.....	20
5. Grain size distribution.....	21
6. Sample soil for consolidation (a) Clay sample in the ring and (b) apparatus used for consolidation .....	22
7. Void Ratio - Log (P) Consolidation curve.....	22
8. The procedure of installing a Shelby tube .....	23
9. Sample of the UU results for (a) model 1 soil and (b) model 2 soil.....	24
10. UU test Sample .....	25
11. Steel tank model.....	26
12. Experimental model setup (a) steel tank (b) prepared soil and (c) used steel plate.....	26
13. Piles installation procedure .....	28
14. Thermocouples distribution on piles and in soil.....	29
15. Pullout system setup .....	32
16. Temperature variation during 2U-Pile cycles at 80 mm depth.....	34
17. Temperature variation during 2U-Pile cycles at 400 mm depth.....	34
18. Temperature profiles at the end of heating phases for 2U-Pile .....	35
19. Thermal exchange rate around the 2U-Pile .....	36
20. Temperature variation during S-Pile cycles at 80 mm depth.....	37

21. Temperature variation during S-Pile cycles at 400 mm depth.....	37
22. Temperature profiles at the end of heating phases for S-Pile .....	38
23. Thermal exchange rate around the S-Pile .....	38
24. Soil temperature distribution along radial distance from the piles' surfaces.....	39
25. Variation of thermal exchange rate of the geothermal piles during heating.....	40
26. The three piles uplift test results .....	42
27. Temperature variation during 2U-Pile cycles at 80 mm depth.....	47
28. Temperature variation during 2U-Pile cycles at 400 mm depth.....	47
29. Temperature profiles at the end of heating phases for 2U-Pile .....	48
30. Thermal exchange rate around 2U-Pile during the three cycles.....	49
31. Temperature variation during S-Pile cycles at 80 mm depth.....	50
32. Temperature variation during S-Pile cycles at 400 mm depth.....	50
33. Temperature profiles at the end of heating phases for S-Pile .....	51
34. Thermal exchange rate around S-pile .....	52
35. Thermal exchange rate during cycles .....	52
36. Variation in load during 2U-Pile cycles .....	53
37. Variation in pile head displacement during 2U-Pile cycles.....	54
38. Variation in load during S-Pile cycles .....	54
39. Variation in pile head displacement during S-Pile cycles .....	55
40. Soil temperature distribution along radial distance from the piles' surfaces.....	56
41. The thermal exchange of the two piles during heating cycles .....	57
42. Head displacement as a function of temperature for 2U-Pile.....	58
43. Head displacement as a function of temperature for S-Pile.....	58
44. The three piles uplift test results .....	60

45. Comparison of the temperature distribution in soil around pile for during heating in E1 and E2 at depth 80 mm for (a) 2U-Pile and (b) S-Pile and at 400 mm for (c) 2U-Pile and (d) S-Pile .....	62
46. Comparison of the thermal exchange of the energy piles in the two experimental tests for (a) S-Piles and (b) 2U-Piles.....	63
47. Pile head displacement and thermal expansion of the pile during cycle of S-Pile .....	65
48. S-Pile cycles results (a) total pile head displacement during heating phase (b) total plastic deformation at the end of each recovery phase (c) maximum reached temperature difference during cycles and (d) duration of each cycle .....	66
49. Variation of plastic displacement per unit time at the end of each cycle .....	67
50. Recovered pile head displacement and thermal pile expansion .....	68
51. Schematic of the model used in Plaxis .....	70
52. Boundary conditions: (a) mechanical and (b) thermal.....	72
53. Stress displacement curves .....	73
54. Temperature variation with time during experimental and numerical analysis at 80 mm depth.....	75
55. Temperature variation with time during experimental and numerical analysis at 400 mm depth.....	75
56. Numerical and experimental (S-Pile) temperature difference (with ambient) variation at horizontal distance .....	76
57. Temperature variation in soil at the end of heating phase in Plaxis 2D .....	77
58. Temperature variation in soil at the end of cooling phase in Plaxis 2D .....	77

## TABLES

Table	Page
1. Properties of different geothermal heat exchange fluids. ....	10
2. Uplift test result during E1 and E2 .....	64
3. Modeled soil characteristics.....	73
4. Thermal properties of soft clay .....	74

# CHAPTER I

## INTRODUCTION

### **1.1 Introduction and Background**

The environment is constantly changing, and the nations are increasingly becoming aware of the problems that surround this change. Of these problems, global warming has become a certain fact about our current situation, which is warming up the planet. These environmental problems have made the world vulnerable to disasters and tragedies. In the United States of America (USA), electricity generation is the largest source of air pollution, in which buildings consume 70 % of its electricity and generate 43 % of USA carbon emissions. All these environmental problems, in addition to other factors such as geopolitical disputes (1973 oil crisis) lead the world to start reconsidering renewable substitutes.

The Renewable Energy Directive, a European Union directive, established an overall policy for the production of energy from renewable sources in the European Union (EU). It requires the EU to fulfil at least 20% of its total energy needs with renewables by 2020, to be achieved through the accomplishment of individual national targets. The Directive specifies national renewable energy targets for each country, considering its starting point and overall potential for renewables. These targets range from a low of 10% in Malta to a high of 49% in Sweden.

One widely utilized renewable energy source is geothermal energy. It is a clean and sustainable energy source. Geothermal energy is the second most abundant source of heat on earth, after solar energy. It is the natural heat energy stored in the earth.

Below a depth of 10–15 m, the ground temperature is constant throughout the year and approximately equal to the mean annual air temperature.

For tens of thousands of years, geothermal water from natural pools and hot springs has been used by humans for cooking, bathing and heating. The Romans used geothermal energy for space heating, and direct heating has been used universally for agricultural purposes for many years, for example greenhouse heating.

In the 21<sup>st</sup> century, renewable energy has become more accessible and its significance has grown in the design of more energy efficient buildings. The first applications of heat exchange via foundation elements were in Austria and Switzerland; shallow foundation elements such as ground bearing slabs and shallow basement walls were first utilized for energy exchange, and these were quickly followed by bearing piles (mid-1980s), diaphragm walls (mid-1990s) and then tunnels (early-2000s) (Brandl, 2006<sup>2</sup>). The benefit of using this approach is that it takes advantage of the structural piles that were already slated to be built, thus reducing the costs of installing the geothermal system. Nowadays, worldwide energy piles popularity is constantly growing and in Austria there are more than 100 000 of units installed (Brandl, 2013)<sup>3</sup>. Heat exchanger piles utilize heat energy stored in the ground to provide a reliable and effective means of space heating and cooling. In winter, with the aid of a heat pump, when the water is colder than the soil, heat is removed from the circulating fluid (and indirectly extracted from the soil) and renders a higher temperature to the heating. Whereas, in summer, conversely, when the water is warmer than the soil, heat is dissipated into the soil for cooling.

Temperature effects have been shown to be significant in many geotechnical engineering problems, such as landfills, pipelines, pavements, buried power cables,

ground energy storages, and the storage and high-level radioactive waste repositories. Indeed, any analysis of the interaction between the ground and the atmosphere must take into account temperature effects and energy exchange (Blight, 1997)<sup>4</sup>.

Over the past twenty years, significant interest has been generated in the potential for using energy piles. Many researchers have studied the topic from various perspectives and for a variety of possible applications. The areas of inquiry included the evaluation of thermal resistance of the pile, its thermal behavior, the response of the surrounding soil that is subjected to thermo-mechanical loading, and measures/approaches towards increasing thermal efficiency. In particular, the question of possible thermal effects on the mechanical properties of the surrounding/supporting soils has been central to some of the leading research efforts. Published work on energy piles shows that in granular and very stiff, moderately to highly overconsolidated clayey soils, thermal effects may be neglected. However, in normally to slightly overconsolidated clays, heating may induce flow of water around the pile and could thus affect the skin friction and the adhesion between the pile and the clay.

When a thermal load is applied to the soil surrounding a structure, a pore water pressure rise will generally result from the increase in temperature due to the fact that the thermal expansion coefficients of the pore water and soil particles are different. The increase in pore water pressure may be significant and may even result in thermal failure of soils (Gens, 2010)<sup>4</sup>. On the other hand, during cycles of heating and cooling, pile expands and contracts, respectively. The rate of contraction after expansion for the pile is different from that of the soil, which may create a gap at the soil-structure interface.



Thermal efficiency of the system is also a subject of significant interest and importance. A number of variables, such as heat exchange fluid, tubing material, and exchange loop configuration, affect the efficiency of such systems and thus have been the subject of exploration and research to optimize energy extraction/ release from/to the subsurface strata. Typical configurations consisted of single or multiple U-shaped tubing, or W-shaped tubing. Recently researchers suggested that increasing the contact area between the pile and the tube might increase the thermal flow rate and as a result, increase the effect on the temperature of the surrounding soil.

This research aimed to investigate the thermal behavior of soils, the effects of cooling/heating cycles on the skin friction of energy piles in slightly overconsolidated clays, and the thermal efficiency of different loop configurations, by carrying out two laboratory experiments. Whereas ideally full-scale tests on energy piles would be desirable, 1-g models in the laboratory, offer an interesting and very useful tool for research. These are designed at a scale, which allows for the development of the relevant phenomena and stress levels. Another major advantage of model tests, like those described in this paper, is that multiple tests can be performed under fully controlled testing conditions, avoiding uncertainties of natural soil profiles. Like any other experimental method, they have some disadvantages, such as staying in low-stress ranges and lack of scale factors for generalizing the results obtained via a little model to a prototype.

To further study the behavior of energy piles, the results of the experimental testing were used to build a numerical model. Due to the complexities of the coupled equations and boundary conditions, the finite element (FE) method has been considered as an appropriate tool to solve the coupled problems associated with thermal issues.

Plaxis 2D Thermal was used to create the model, validate it, and use it further to study the effect of different parameters of the thermo-mechanical response.

## **1.2 Literature Review**

### ***1.2.1 Energy Pile***

Energy pile, shown in Figure 1, is a structural element that aside its primary function, carrying the structure load, it has a secondary function. This function is to exchange heat between the building and the ground. This happens by circulating a fluid (water or antifreeze) through tubes embedded in the piles. During summer, the energy pile acts as heat sink by storing the excess heat from the structure in the ground.

However, during winter, the process is reversed, and the energy pile acts as heat source by extracting energy from the subsurface layers and released in the assembly.

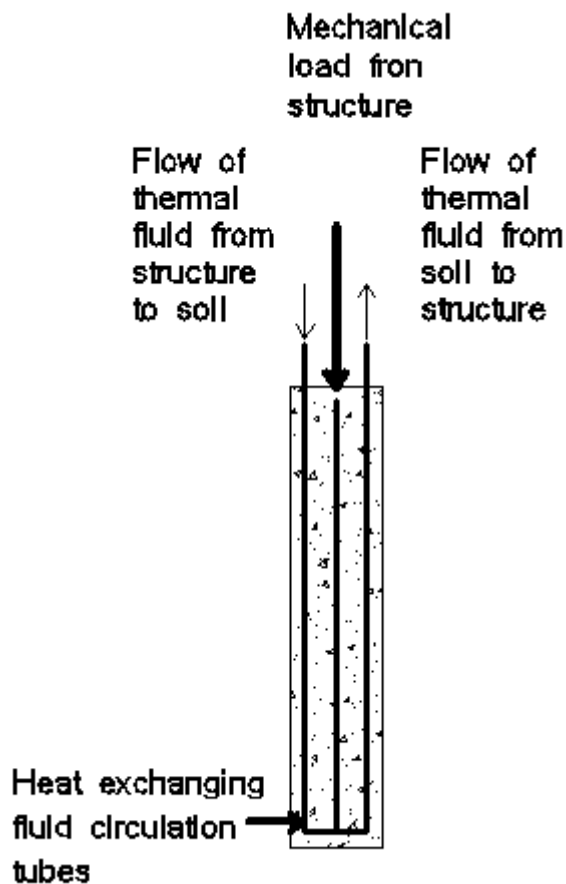


Figure 1. Schematic view of a geothermal energy pile

### 1.2.2 Energy Pile: Types and Benefits

There are several types of energy piles used across the world, that depends on the manufacturer, available resources, and installation technique. These usually are steel or concrete because they are both capable of carrying a tremendous amount of weight. The latter is the most common in the region and the type considered for this laboratory experiment.

Energy pile comprises a great substitution for traditional heating and cooling means, contributing to environment protection. In addition, it is applicable in most climates and regions. Although energy piles may not provide the full amount of energy

required to heat and cool residential and commercial buildings, they may provide sufficient heat exchange to cover the base heating and cooling load for the building, which is typically 10–20% of the peak heating or cooling load. In this case, a conventional heating or cooling system would not be required except during peak heating or cooling events (C. G. Olgun & J. S. McCartney 2014)<sup>5</sup>.

### ***1.2.3 Thermal Response***

#### ***1.2.3.1 Configurations***

The thermal performance of energy piles has also been widely studied to improve their design as geothermal heat exchangers. Energy pile is characterized by having embedded tubing to allow the fluid to exchange heat by circulating in it. This tubing can be installed as single U-tube, double U-tube, multi U-tube, W-tube, or Spiral-tube as shown in Figure 2.

For different types of heat exchanger piles, research is only focused on thermal response, but much less on thermomechanical response. Because of the large difference in heat transfer performance and different amounts and placements of pipe in the piles (Gao et al., 2008<sup>6</sup>; Hamada et al., 2007<sup>7</sup>), the thermo-mechanical behavior is different. Many experimental and numerical studies investigated the difference in thermal efficiency of the system when varying the tubing configuration (Hamada et al., 2007, Jalaluddin et al., 2011<sup>8</sup>, Luo et al., 2016<sup>9</sup>, Gao et al., 2008).

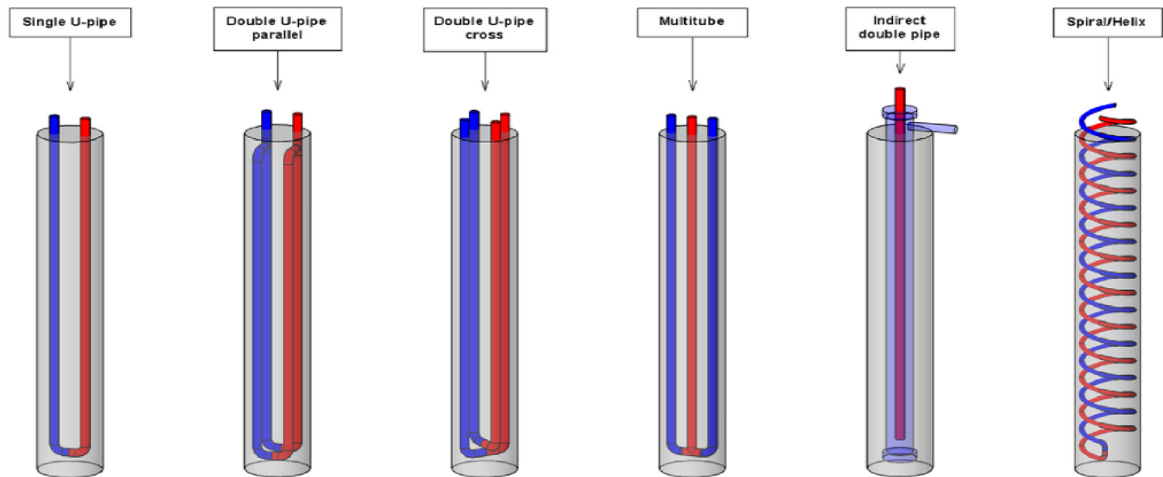


Figure 2. Different heat tubing configurations

Studies of different heat exchange loops showed that specific heat extraction or rejection rate increases with the increase of the tube surface area in contact with the pile. However, high heat extraction/ rejection potential may not be optimal solution in a long run, as the amount of potential ground extracted energy depends also on ground initial temperature and ground source system application, heating or cooling (Fadejev et al. 2017)<sup>10</sup>.

Jalaludin et al. (2011) reported that the heat exchange rate is higher for the double-tube arrangement as compared to either the multi-tube or the single U tube setup. Luo et al (2016) indicated that the triple U-shaped tube had the best thermal performance after running thermal performance tests on different types of ground heat exchangers and numerical modelling under intermittent\cycled conditions.

Batini et al. (2015)<sup>11</sup> observed that the W-shaped pipe configuration resulted in an increase of up to 54% in the heat transfer rate compared with the single U-shaped configuration at the same flow rate. The double U-shaped pipe configuration, which possessed a double flow rate with respect to the other configurations, resulted in the highest cooling of the concrete with the greatest related stress and displacement

distributions. Therefore, it was considered a less advantageous solution with respect to the W-shaped pipe configuration from both a thermo-hydraulic and a geotechnical point of view. Wang et al. (2017)<sup>12</sup> concluded that W-tubing heat exchanger resulted in the largest variations in pile and soil temperatures, while the S-tubing had the next best performance.

#### 1.2.3.2 Soil and Fluids Characteristics

To optimize the design of a geothermal system, the thermal response is evaluated accurately. This is done by knowing the thermal conductivity of the material of the pile used and the soil surrounding it and by choosing the adequate heat exchange fluid and its rate.

There are several factors that affect the thermal conductivity of the soil, including density, water content, and quartz mineral content, such that quartz crystal has one of the highest thermal conductivity values among minerals.

As for the heat exchanger liquid, it is chosen mainly according to the expected temperatures reached by the system, these fluids can be, water, ethylene glycol, propylene glycol, and methanol. In general, these fluids are mixed with water to some proportion to create an antifreeze solution due to their significantly low freezing points as shown in Table 1. In addition, the flowrate is an important factor to attain the optimal heat exchange. The fluid flowrate should be sufficient to have a turbulent flow in the pipes embedded in the pile.

Table 1. Properties of different geothermal heat exchange fluids.

Properties	Freezing Point (F)	Normal Boiling Point (F)	Thermal Conductivity (W.m/K)
Water	0	100	0.609
Ethylene glycol	-13	197	0.258
Propylene glycol	-59	188	0.147
Methanol	-98	64	0.202

#### ***1.2.4 Experimental Research***

Several studies have highlighted the importance of gaining better understanding of coupled loading conditions and temperature effects on the soil pile interaction mechanism. For this purpose, a significant research effort has been invested worldwide to investigate soil-pile interaction using laboratory scale 1-g tests, centrifuge tests, and full-scale field tests (Brandl 2006<sup>2</sup>; Laloui et al. 2006<sup>13</sup>; Bourne-Webb et al. 2009<sup>14</sup>; McCartney and Rosenberg 2011<sup>15</sup>; Amatya et al. 2012<sup>16</sup>; McCartney and Murphy 2012<sup>17</sup>, Akrouch et al. 2013<sup>18</sup>, and Stewart and McCartney 2014<sup>19</sup>). Bourne-Webb et al. (2016)<sup>20</sup> summarize several research studies that have investigated the load transfer mechanism in thermally-activated piles. All the reported thermo-mechanical load tests concluded that the use of energy piles induces change in the stress and strain and load redistribution in the pile element itself.

Of particular significance is the effect of temperature cycles on side friction as it has been postulated that contraction during cooling and/or cycles of heating and cooling may lead to a decrease in side friction. In granular and very stiff, moderately to highly overconsolidated clayey soils where the soil response is more likely to be elastic, it was found that thermal effects on the mechanical properties of the soils may be neglected. However, in normally to slightly overconsolidated clayey materials, this may

not be true because heating may induce water flow leading to thermal consolidation of the soil, with possible effects on the side friction. McCartney and Rosenberg (2011)<sup>15</sup> state that the possible adverse effects of cooling and heating on skin friction of energy piles in clay has not been fully investigated. Evidence of a thermal softening effect on the shear strength of clay was also presented by Uchaipichat and Khalili (2009)<sup>21</sup> who emphasized the need for research in this area.

Yavari et al. (2016)<sup>22</sup> studied the mechanical behavior of an energy pile in saturated clay under thermo-mechanical loading and found that irreversible settlement of the pile head is observed after the heating/cooling cycle under constant pile head axial load. This settlement is larger under higher axial loads and is much more significant than that due to creep under isothermal conditions.

Ng et al. (2014)<sup>23</sup> investigated the effects of heating/cooling cycles on the long-term displacement of an energy pile in lightly and heavily overconsolidated kaolin clay. A ratcheting settlement was observed due to the cycles in both types of soil, however, in heavily overconsolidated clay, the ratcheting displacement pattern had smaller magnitude. The paper suggested that it is because clay with a higher OCR tends to have less contraction.

The reported tests on energy piles are generally compression tests where both vertical-side shear and point/tip resistance are engaged during loading. In addition, most of the published field scale tests involve granular soils. The only exceptions are the tests by Akrouch et al. (2013) and Bourne-Webb et al.(2009). Bourne-Webb et al. (2009) noticed a significant effect of high temperature on the pile shaft resistance in London clay. Akrouch et al. (2013) performed tension load tests on energy piles in high plasticity stiff clay after thermal cycling loading for five days under different



mechanical load levels to investigate their time-dependent performance. The results showed that the increase in soil-pile temperature leads to an increase in the creep rate and long-term displacement that should be taken into account when designing energy piles.

### ***1.2.5 Numerical***

The numerical methods of analysis have been applied to the analysis of energy piles either to back-analyze field and laboratory tests behavior of particular features; thermal response, thermal efficiency or effect on soil-structure interaction, or to further study the effect of certain parameters on the behavior of these piles.

Numerical analyses (primarily FEM-finite-element method) have been employed by Laloui et al. (2006), Di Donna and Laloui (2015), Rotta Loria et al. (2015), Bourne-Webb et al. (2016) and Di Donna et al. (2016), among others to further explore/understand the complex interaction involved and their effects on piles behavior. It should be noted that these numerical analyses vary in complexity in terms of both the finite-element formulation and the modelling approach. Ozudogru et al. (2015) implemented a finite element method that focuses on the pile-soil interface without simulating the heat transfer in the soil. Yavari et al. (2014b) and Yavari et al. (2015) performed uncoupled analyses where the soil was modelled as linear elastic–perfectly plastic. Abdelaziz and Ozudogru (2016) combined the finite-element method, to simulate the heat transfer in the pile and the soil, with the load transfer approach, to approximate the thermal stresses.

Knellwolf et al. (2011), McCartney and Rosenberg (2011) and Suryatriyastuti et al. (2014) used the load transfer (t-z) approach, which includes the effect of thermal expansion and contraction of the pile.

Bourne-Webb 2013<sup>24</sup> indicated that the thermo-mechanical response varies as a function of the temperature applied and the physical restraints a pile subjected to. A free pile will be able to deform freely with minimum stresses, while a fully restrained pile will have an alteration in the axial stresses in proportion to the temperature change. These two extremes of perfect freedom and fixity impose bounds on the thermal response of the pile shaft.

Fuentes et al. (2016)<sup>25</sup> studied the thermal effect on the shaft friction of the geothermal piles under different values of soil compressibility, permeability and temperature using finite difference method. Their research concluded that, increasing temperature, lowering permeability or increasing compressibility of soil results in greater excess pore water. In addition, it identified a shaft resistance reduction factor to allow the calculation of developed pore water pressures in terms of the shaft bearing capacity of geo-piles.

Khosrasvi et al. (2016)<sup>26</sup> investigated the thermo-mechanical behavior of energy piles under the effect of head-structure stiffness, by applying vertical loads,  $P$ , and soil properties, soil's Young modulus  $E$ , using finite difference method. It revealed that increasing the vertical load applied to the pile head resulted in a larger thermal axial stress at the top of the pile and a decrease in the strain along the pile. However, no change in behavior was observed at the toe of the pile. In addition, the graphs showed that the null point moved upward as the head restraint increased. Similar trend was observed when varying the soil stiffness. The numerical results displayed that the

thermal axial stress increased, and the thermal axial strain decreased with the increase of the soil's Young modulus.

Klementyna et al. (2016)<sup>27</sup> tested the effects of the modelling approach, the thermal load application, thermal conductivity and permeability of the soil using finite element model. The pile was initially loaded to 1200 kN, followed by a 1-year cycle comprising 6 months of energy extraction and 6 months of injection. Not simulating consolidation gave the greatest head displacement and under predicts the changes in axial stresses. However, not simulating heat transfer in the soil yielded the smallest head displacement and overestimation for the changes in axial stress. Changing the thermal load from constant temperature to heat flux did not have a significant impact and can be ignored. It also revealed that lower soil thermal conductivity induced higher axial stress change and lower permeability resulted in larger displacement of pile head.

### ***1.2.6 Design of Energy Piles***

Despite the wide use of energy piles across the world, there is no official standards to guide the design of these structures. However, some professionals and experts produced guidance documents to organize the utilization and design of energy structures.

Bourne-Webb et al.<sup>20</sup> summarized the main performance criteria to consider in design, serviceability and possibility of failure. Thermal performance is assured by studying the energy delivered, efficiency of the system, system temperatures, and environmental impact. Energy pile is designed to deliver a certain proportion of the buildings heating and cooling requirements with a 10 % margin between required and expected energy supply. The system's efficiency must match the EU Renewable Energy

Sources Directive requirements. System temperature is chosen within limits, lower bound of 2 °C, to avoid ground freeze and upper bound of 40 °C, to maintain pump's efficiency. Environmentally, the increase in the development of such systems may lead to interaction between adjacent systems that must be further considered.

In addition to thermal performance, Bourne-Webb et al. explained mechanical performance by three criteria; deformations, overstress, and resistance. Observed contraction and expansion of piles due to heating and cooling resulted in pile head movement in the order of 40 to 60 % of the theoretical maximum values, for a free-standing column. These deformations are accounted for on a case-by-case basis. Experimental studies showed an internal stress changes between 50 and 100 % of the theoretical value for a perfectly restrained column, thus these changes are considered to ensure an adequate margin between expected and ultimate resistance of the material. Finally, strength and volume change characteristics of the ground may be altered due to temperature change, and cyclic expansion and contraction may lead to further alterations in the available resistance and stiffness, which requires further investigation to have a better understanding of the risks accompanied with it and a better method to integrate it with design.

### **1.3 Thesis Objectives and Significance**

#### ***1.3.1 Objective and Scope***

Energy piles are considered a relatively new “technology” that is finding increased interest and acceptance. This increased the need for improved scientific knowledge of their behavior. The effects of temperature changes on the response of these structures represent a challenge for geotechnical and structural engineers because

they induce thermal expansion and contraction of both the piles and the surrounding soil as well as modifications to the stress state.

Since the effect of temperature changes on the behavior of soil is of interest in a number of fields, several efforts have been devoted to the investigation of thermal effects on granular and very stiff, moderately to highly overconsolidated clayey soils. However, the effect on normally to slightly overconsolidated clays has not been fully investigated. Therefore, this study presents the results of a laboratory scale experimental program that was designed to explore some of the aforementioned gaps/limitations in the literature.

The objectives of this study are to (1) investigate the effect of heat exchange on the skin friction of energy piles that are embedded in normally to slightly overconsolidated clay with and without a sustained load and (2) study the thermal performance of energy piles with two different tubing configurations (Double-U and Spiral) as shown in Figure 1.

#### 1.3.1.1 Laboratory Experiments:

The objectives were achieved through (1) two lab-scale experimental models and a (2) numerical finite element model as will be discussed below. The experimental models were piloted using three model concrete piles embedded in a saturated soft clay tank with dimensions 1m x 1m x 1.2m. Two of these piles were energy piles, each with different combination of heat exchanging tubes (S-shaped and 2U-shaped), while the third was a control pile that was not subjected to any heating/cooling cycles. In the first experimental testing, the two energy piles were subjected to thermal cycles, and the three piles were pulled out to investigate any variation in their skin friction. During the

second experimental testing, the same procedure and experimental material were used but with two variables. The first difference was subjecting the three piles to a tension loading that comprises 30 % of the ultimate capacity of the piles that was evaluated during the first experiment. The second difference is subjecting one of the energy piles to additional thermal cycles to study its long-term effect.

#### 1.3.1.2 Coupled Simulations using PLAXIS

In parallel with the experimental testing, a numerical model was implemented using the finite element software Plaxis 2D. Axisymmetric model with coupled thermo-hydro-mechanical analyses was executed in this proposed study. First, the experimental setup was modeled, and then the results were compared to validate the model of the software.

#### ***1.3.2 Significance***

Geothermal Piles can potentially provide an eco-friendly cost-effective source of ground energy, and reduce CO<sub>2</sub> emissions while providing renewable energy for cooling and heating. They serve a dual function as both structural components of the foundation system as well as an energy source/sink which is incorporated into the building's energy balance. There is currently lack of knowledge on the effect of cooling and heating cycles on the skin friction of energy piles in slightly overconsolidated clays. The work in this thesis is specifically targeted to cater for this need. In addition, the work intends to explore the efficiency of various configurations of the embedded heat exchange loops. The results of the proposed study will contribute to expand the knowledge and confidence in dual purpose piles for structural support and energy efficiency

## **1.4 Thesis Organization**

This thesis is organized in the following way:

Chapter 1 presents an introduction and literature review on energy piles.

Chapter 2 describes the experimental setup of the testing.

Chapter 3 includes the procedures and results of Experimental Model I (E1).

Chapter 4 includes the procedures and results of Experimental Model II (E2).

Chapter 5 presents the analysis of the experimental testing results.

Chapter 6 includes the finite element analysis using Plaxis 2D.

Chapter 7 presents the conclusions of the research work.

## CHAPTER II

### EXPERIMENTAL SETUP

#### 2.1 Model Piles

The setup included three piles, two of which are geothermal piles and one is a control pile. The three were concrete piles, having a compressive strength of 32 MPa, diameter of 120 mm and length of 600 mm. The concrete mixture was prepared according to the normal Portland cement guidelines, so each pile composed of 9 kg of coarse aggregate, 3.5 Kg of cement, 5.75 Kg of sand, and 2 L of water.

Figure 3. Model piles (a) S-Pile (b) C-Pile and (c) 2U-Pile

Both geothermal piles included tubing made of copper of 4 mm inner diameter, while the third is a control pile with no copper tubes embedded (C-Pile). The two geothermal piles had different configurations; the first had S-shaped tubes (S-Pile), while the second had two U-shaped loops (2U-Pile), as shown in Figure 4.



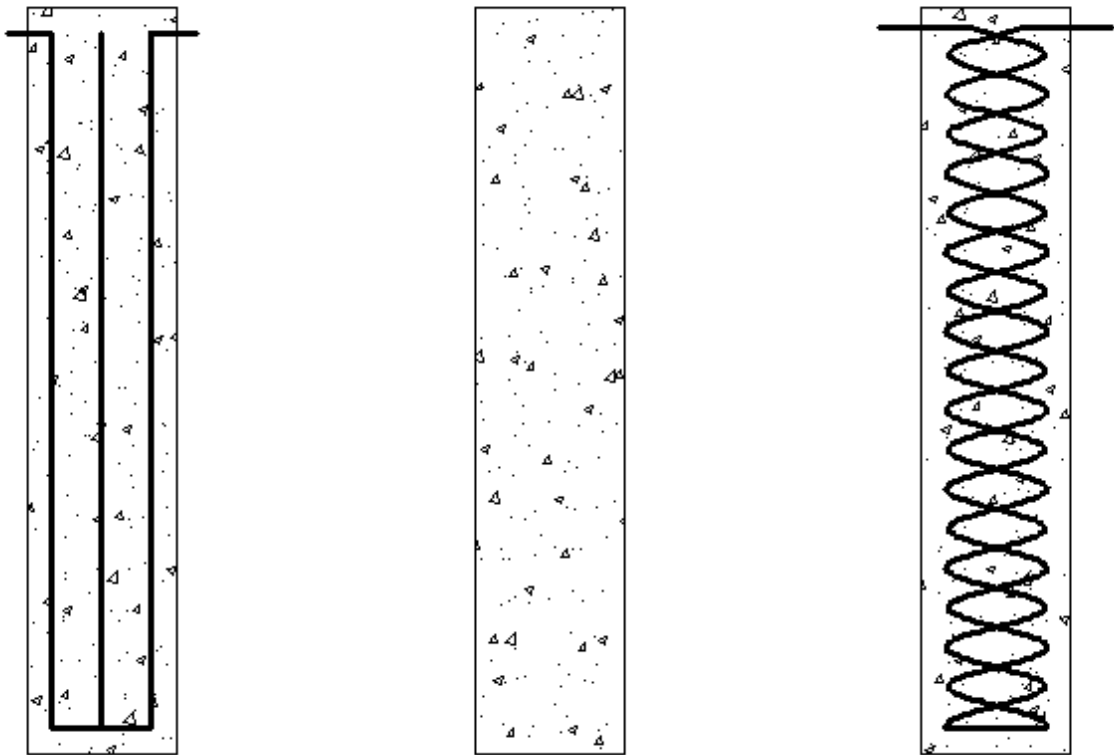


Figure 4. Configurations of the piles (a) 2U-Pile (b) C-Pile and (c) S-Pile

## 2.2 Soils Tests

The literature included many testing over sand, but few discussed the effect of thermal energy in thermal piles on clay. Thus, clay was the testing subject.

The clay specifications were characterized through several laboratory tests, following the American Society for Testing and Materials (ASTM) standards. Initially the soil was sieved on sieve number 10 (2 mm),

First a specific gravity test of Soil Solids by Water Pycnometer was done to give  $G_s = 2.6$  in which the specific gravity of a given material is defined as the ratio of the weight of a given volume of the material to the weight of an equal volume of distilled water. Then a sieve analysis and hydrometer test were conducted to classify

the grain sizes in the soil. The results illustrated in Figure 5 shows that the soil constitutes of 25.3 % sand and 74.7 % fines. The fines are divided 34.7 % clay and 30 % silt.

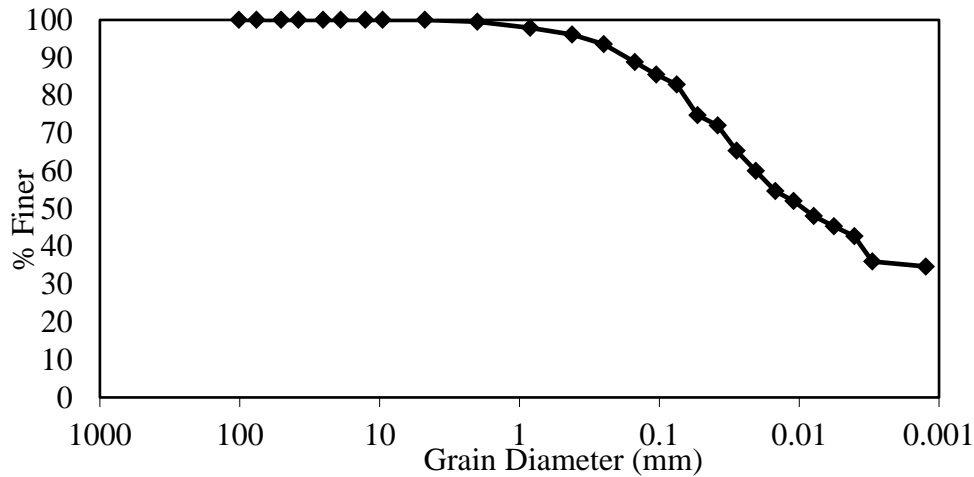


Figure 5. Grain size distribution

Atterberg limit analysis was done to define the properties of the soil liquid limit and plastic limit. The liquid limit (LL) is defined as the moisture content at which the soil begins to behave as a liquid material and begins to flow and it was determined using the Casagrande apparatus. It was found to be 28.9 %. The plastic limit is defined as the moisture content at which soil begins to behave as a plastic material. The plastic limit (PL) is the water content, in percent, at which a soil can no longer be deformed by rolling into 3.2 mm (1/8 in.) diameter threads without crumbling. It was found to be 16.4 %.

In addition, a consolidation test was conducted on the sample to evaluate the coefficient of consolidation ( $C_v$ ) over the following stresses: 8, 15, 20, 30, 40, 80, 160, 80, and 40 kPa as shown in Figure 7. It was decided to consolidate the soil with 20 kPa stress so the coefficient of consolidation for this stress is  $C_v = 0.0366 \text{ mm}^2/\text{s}$ .

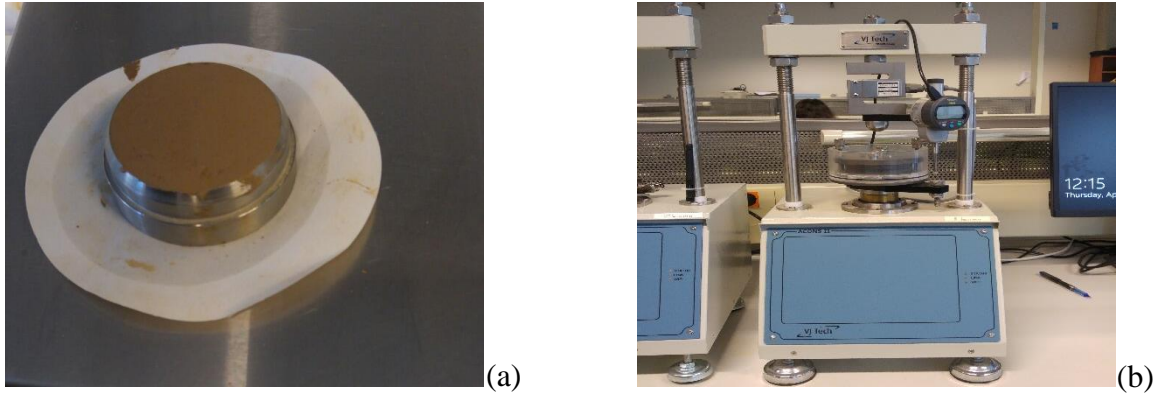


Figure 6. Sample soil for consolidation (a) Clay sample in the ring and (b) apparatus used for consolidation

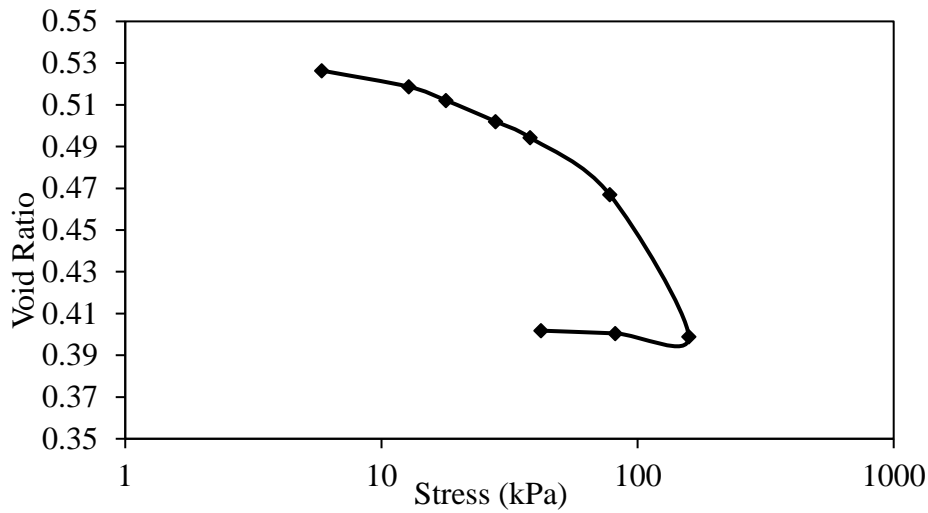


Figure 7. Void Ratio - Log (P) Consolidation curve

Then another consolidation test was conducted after consolidation for both experimental models to get ~19 kPa as preconsolidation stress ( $\sigma'_p$ ), 0.13 compression index ( $C_c$ ), and 0.02 swelling index ( $C_s$ ).

Three Shelby tubes were used to sample the clay from the locations at which the piles were intended to be installed during both experiments, E1 and E2 (Figure8). Each Shelby tube allowed for testing three samples using unconsolidated undrained triaxial tests under a confining pressure of 20 kPa.



Figure 8. The procedure of installing a Shelby tube

The average undrained shear strength ( $S_u$ ) for the first model was 14.78 kPa, 13.31 kPa, and 15.68 kPa respectively for the S-pile, C-pile, and 2U-pile, locations, with corresponding average water contents of 22.13 %, 24.43 %, and 22.63%. Whereas, for the second model, the average undrained shear strength was 18.8, 17.7, and 19.2 kPa respectively for the S-pile, C-pile, and 2U-pile locations, with corresponding average water contents of 22.3%, 22.9%, and 22.6%, respectively. The relatively higher water content and lower undrained shear strength in the clay at the location of the control pile (center of the tank) could be attributed to a slightly lower degree of consolidation given the longer drainage path compared to the clay at the locations of the S-pile and 2U-Pile which are located near a drainage boundary at the sides of the tank.

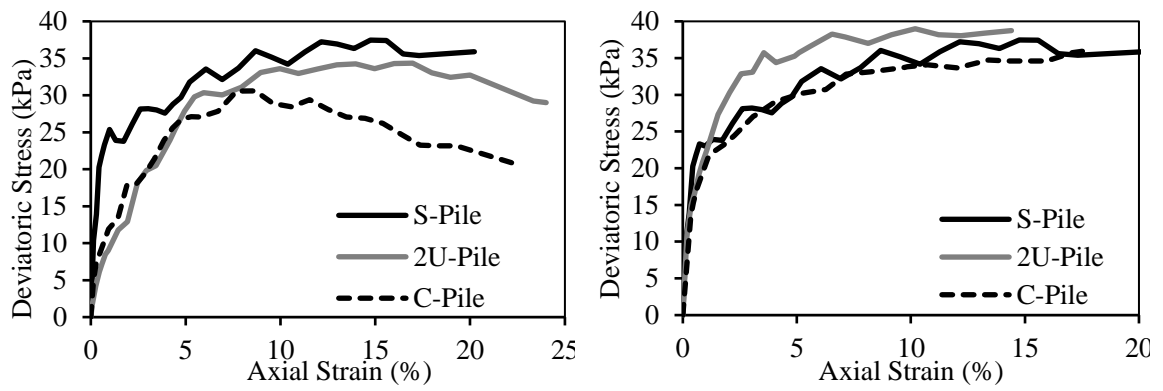


Figure 9. Sample of the UU results for (a) model 1 soil and (b) model 2 soil



Figure 10. UU test Sample

### 2.3 Soil Bed Preparation

A thermally-insulated steel tank with a cross-sectional area of 1000 mm x 1000 mm and a depth of 1200 mm was used in the experiments (Figure 11). The soil used is soft saturated clay. It was prepared in stages with masses of 40 kgs each. It was mixed with water to have a water content as the liquid limit of 28.9 %. Then it was placed in



the tank in 50 – 100 mm layers to have one thick layer of 900 mm thickness. This same procedure was conducted for both experimental models.

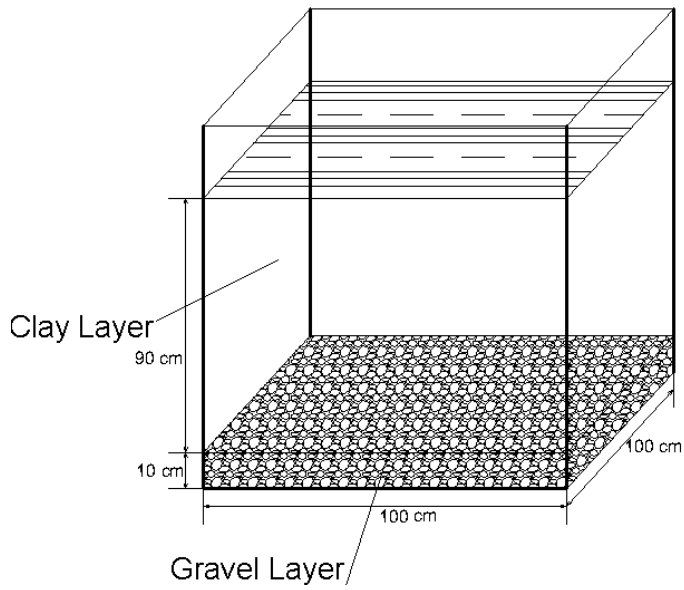


Figure 11. Steel tank model

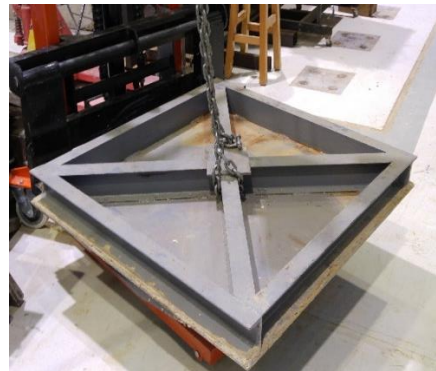


Figure 12. Experimental model setup (a) steel tank (b) prepared soil and (c) used steel plate

Then the soil was consolidated. A rigid steel plate was placed above the soil to distribute the load evenly (Figure 12 (c)). In the first experimental model the steel plate was loaded with dead weights (~ 2 tons) resulting in a uniform applied pressure of about ~19 kPa. However, during the second experimental model, two systems of lever arms were placed facing each other over the steel plate to apply the 2 tons load.

The consolidation process covered a period of 4 weeks for model 1 and 3 weeks for model 2, during which drainage was permitted in both the horizontal and vertical directions through the use of geotextiles that were placed at the sides and bottom of the tank, respectively. Drainage was assured at the base through a gravel layer overlain by the geotextile filter and was evacuated using a faucet that was installed on the lower side of the tank.

#### **2.4 Model Pile Installation**

The three concrete piles were installed using the same method in both experimental models (Figure 13). To install the piles, a hollow PVC tube was used as a temporary casing, with a smaller diameter than the diameter of the piles and with a smooth surface to help extract the inner soil and maintain a sufficient layer of soil to insure good soil-pile interface contact when pushing the piles in the holes. This tube was used to create a stable “temporary hole” into which the model pile could be inserted with good contact and minimal disturbance, given that with the size of the piles (diameter of 120 mm), pushing the piles into the clay bed as prepared would cause large disturbances and generate high pore pressures. After excavating the soil, the PVC tube was extracted, and then piles were inserted via pushing using a hydraulic piston. The



piles were put, with the C-pile at the center to have a sufficient distant between the geo-piles so each pile would not be affected during the cycles of the other.

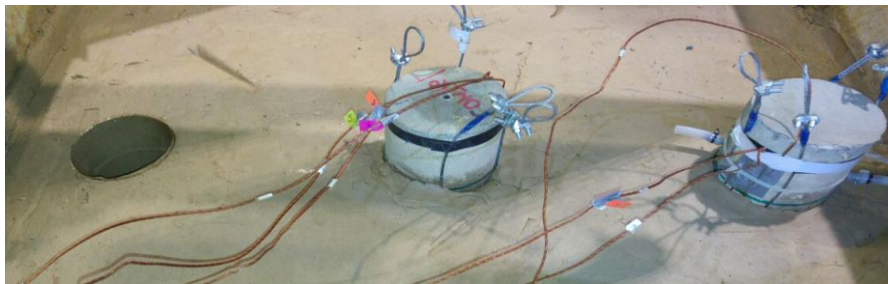


Figure 13. Piles installation procedure

## 2.5 Instrumentation and Data Acquisition

Load, displacement and temperature were examined during the experimental procedures. Load was measured by a load cell (LC) through the uplifts of the piles during E1 and E2, and tensioning during E2. Displacements of the piles were monitored using a Linear Variable Differential Transformer (LVDT) and displacement gauges. The temperatures were monitored using 32 thermocouples that were rearranged with every stage. These thermocouples were distributed at different horizontal distances from the pile surfaces in the soil, at different depths as shown in Figures 3 and 14. Eight thermocouples were attached to the surface of the piles at depths of 80 mm, 250 mm and 400 mm for the geothermal piles and at depths of 80 mm and 400 mm for the control pile. In addition, three thermocouples were installed inside the circulating tubes and outside the tank to monitor inlet, outlet, and ambient temperature. LVDT, LC and thermocouples were connected to an acquisition system to record the variations with time.

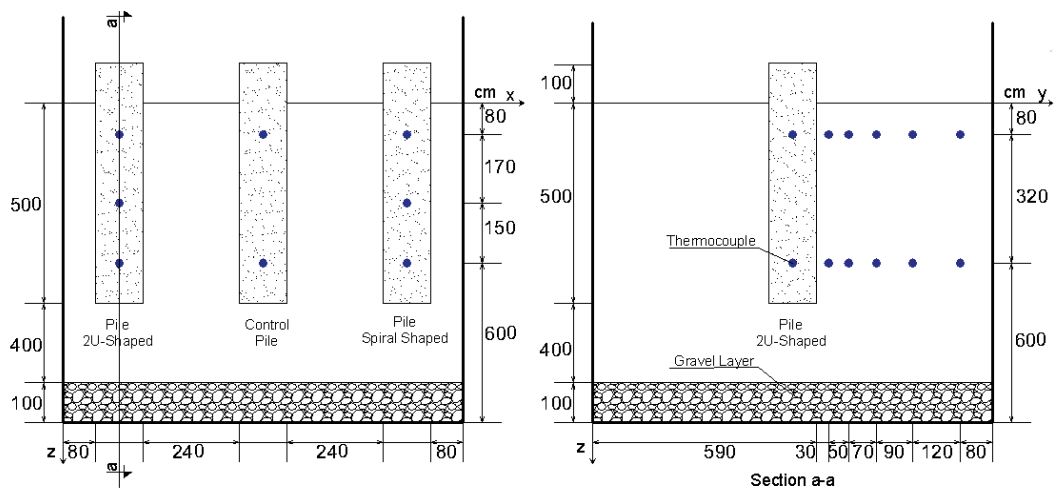


Figure 14. Thermocouples distribution on piles and in soil

## CHAPTER III

### EXPERIMENTAL MODEL I

#### 3.1 Overview

The first experimental model aimed to study the effect of thermal cycles, heating and cooling, on the capacity of the energy piles embedded in slightly overconsolidated clay, the skin friction in particular, by comparing the control pile capacity to that of the two geothermal piles. In addition, having two different configurations of tubing inside the concrete piles permitted investigating the more thermally efficient configuration, by monitoring the temperature variation around the piles.

#### 3.2 Testing Procedure

This experimental model consisted of two stages, thermal cycling and uplift test. The C-Pile was only subjected to an uplift test.

##### 3.2.1 Step 1

The S-Pile was the first pile to be subjected to thermal cycling. These cycles consisted of two phases, heating and recovery. During heating, hot water was pumped from a water bath at a constant temperature 51°C and constant flow rate 260 mL/min. The flow rate was estimated from a Reynold number of 2500 to insure a stable and efficient circulation. It was chosen to assure a turbulent flow using a specific pump, pump head, and tubing. Whereas during recovery, the water pumping stopped, and the

temperature recovered to room temperature. The laboratory ambient day and night temperature was about 22°C.

The pile was exposed to three cycles of heating and recovery. The heating phase's durations were 65 hrs, 18 hrs, and 24 hrs for the first, second and third cycle, respectively. However, the recovery phases lasted for 24 hrs through all cycles.

### **3.2.2 Step 2**

At the end of the cycles, the S-Pile and C-Pile were pulled-out to measure the skin friction. The uplift/pullout tests were conducted using a simple load-controlled system that consisted of two pulleys, a stainless-steel wire, and a set of steel weights that were used to apply the pullout force as shown in Figure 15. The load was applied step-wise in increments that were initially in the order of 50 N and which were reduced in magnitude (to about 5 N) as the pile approached pullout failure. Each load increment was sustained for about 30 seconds to ensure minimal dissipation of pore water pressure during undrained loading. Precise values of the applied load were determined using a load cell that was attached to the wire used to pull out the pile. The corresponding pile movement was monitored using a displacement transducer (LVDT) that was placed at the pile head. The same uplift procedure was adopted for all the testing in E1 and E2.

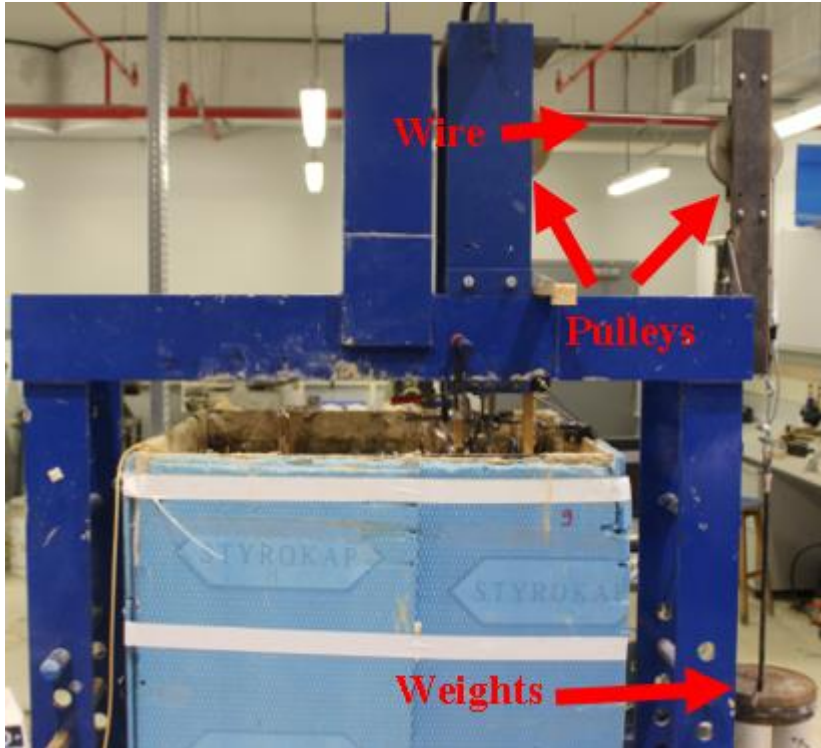


Figure 15. Pullout system setup

### 3.2.3 Step 3

After the uplift tests, heating cycles for the 2U-Pile started. The same sequence of cycle was adopted but the temperature on the inlet was lower, and the maximum reached temperature was 48 °C. During these cycles the temperature on the 2U-Pile and in the surrounding soil was monitored.

### 3.2.4 Step 4

At the end of the three heating/recovery cycles, the 2U-Pile was pulled-out using the same setup to estimate their skin friction.

### 3.3 Results

The temperatures on the surface of the piles and in soil around the piles were monitored during the cycles of the two geothermal piles. The pile head movement and the load during the uplift tests were recorded for the three piles.

#### 3.3.1 C-Pile

The C-Pile was the control pile that was not subjected to any thermal cycles. The pile was pulled-out to be the reference for comparing the mobilized skin friction with that of the geothermal piles. The uplift graph is presented in Figure 26.

#### 3.3.2 2U-Pile

The 2U-Pile was subjected to three heating/cooling cycles and Figures 16 and 17 present the variation of temperature at 80 mm and 400 mm depth, respectively, at different radial distances from the pile surface. The inlet fluid temperature was 48°C. The graphs show an expected trend. During heating, the pile and soil temperatures increased until they reached a steady state, and during cooling, it decreased back to ambient temperature. As expected, the highest values of temperature were at the pile surfaces ~ 43°C while the temperature decreased in the surrounding soil, reaching maximum of 37, 31, and 25°C at 30, 150, and 360 mm horizontal distance, respectively, at 80 mm depth. Whereas the maximum reached temperatures were ~44, 41.3°C, 34.0°C, and 25.5°C, at pile surface, 30, 150, and 360 mm horizontal distance, respectively, at 400 mm depth. The temperature at the pile surface were close, whereas in soil, there was a significant increase with depth. This variation may be due to the atmospheric effect at shallow surfaces. These observations are illustrated in Figure 18.

In addition, as predictable, the temperature decreased with horizontal distance. At 400 mm depth, the temperature decreased 18.5°C between the pile surface and 360 mm away from it.

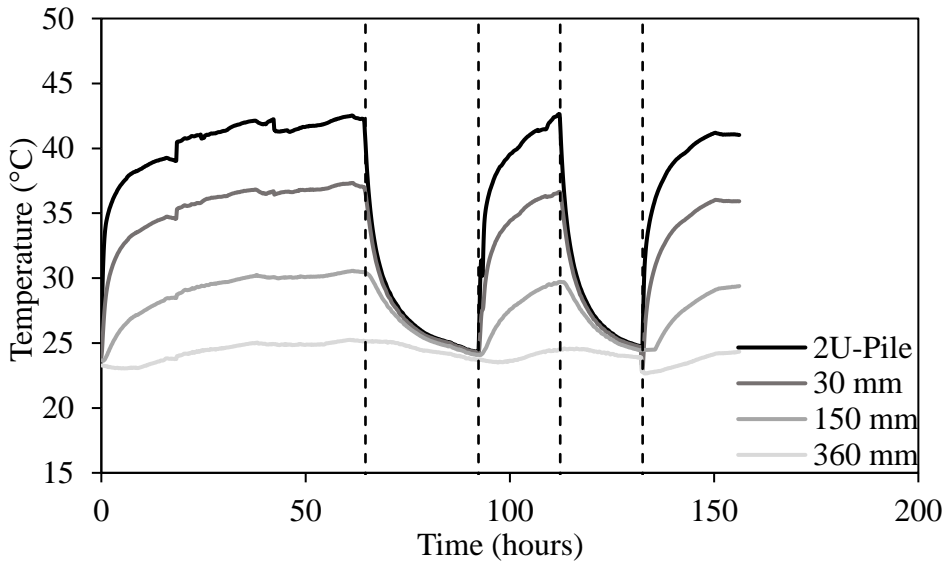


Figure 16. Temperature variation during 2U-Pile cycles at 80 mm depth

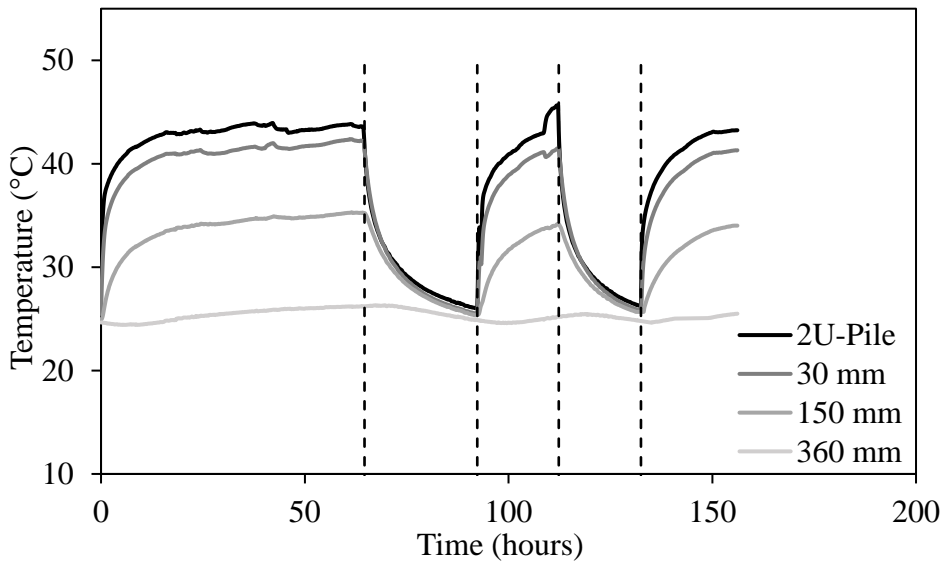


Figure 17. Temperature variation during 2U-Pile cycles at 400 mm depth

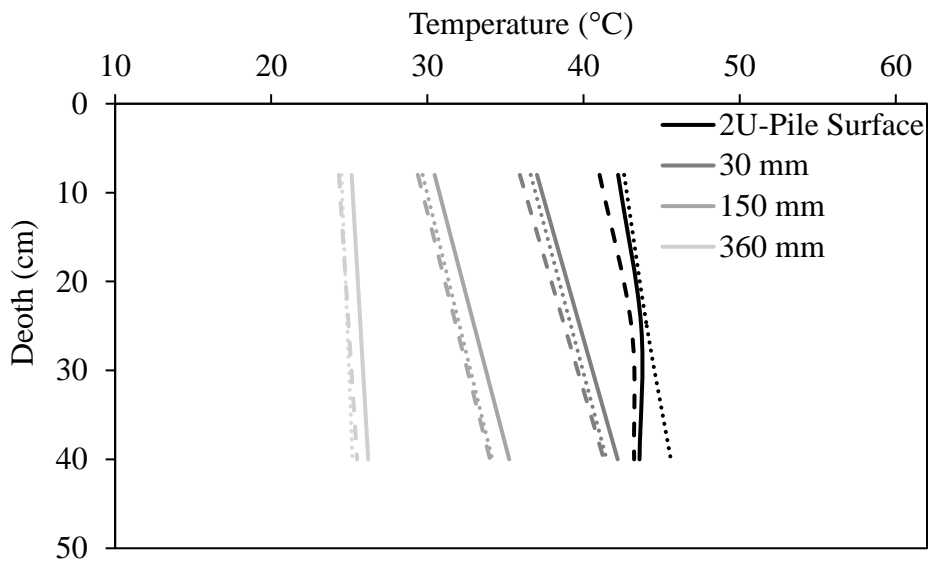


Figure 18. Temperature profiles at the end of heating phases for 2U-Pile

It is not sufficient to compare the change in temperature around the piles to study the different configurations behavior, especially that there was a difference in the initial temperatures. So, to compare the thermal efficiency of the two geothermal piles, their thermal exchange rate per meter length was calculated. The thermal transfer rate,  $Q$ , of an energy pile (W/m) is given by:

$$Q = q C_f \Delta T$$

Equation 1. Thermal exchange rate (W/m).

Where  $q$  is the fluid flow rate ( $m^3/s$ ),  $C_f$  is the volumetric heat capacity of the fluid ( $4.2 MJ/m^3K$ ),  $\Delta T$  is the difference between the inlet and outlet fluid temperature ( $^{\circ}C$ ), and  $H$  is the embedded length of the energy pile (m). The results of the thermal exchange rate, shown in Figure 19, display some fluctuations around an average of 110 W/m.



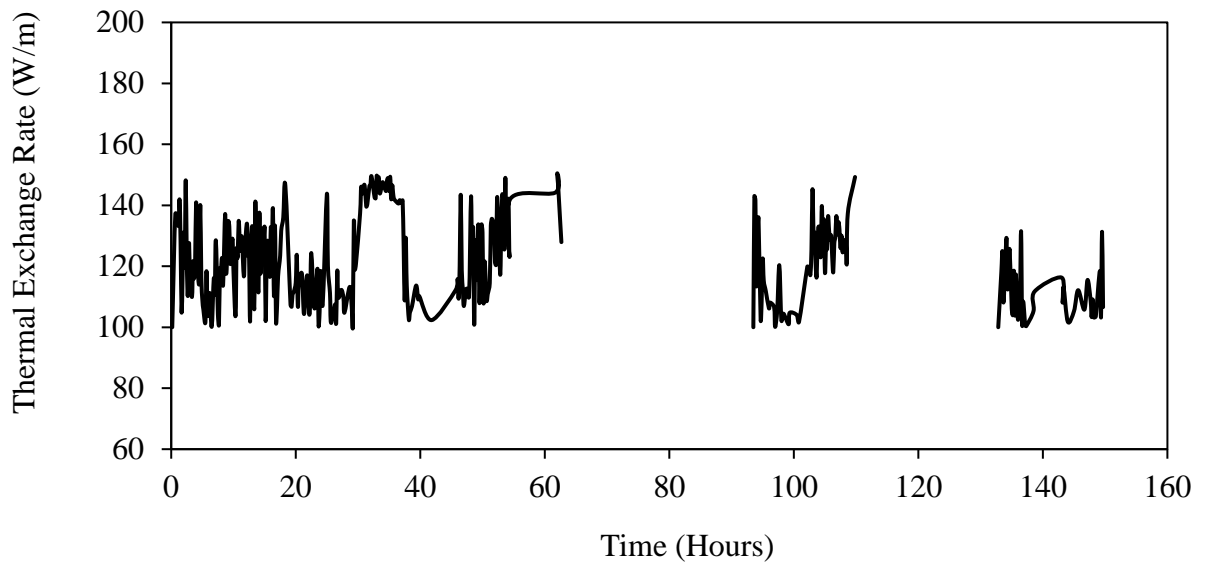


Figure 19. Thermal exchange rate around the 2U-Pile

### 3.3.3 S-Pile

Similarly, the temperatures during the cycles of the S-Pile were recorded at 80, 400 mm vertical depths, and at various horizontal distances and are displayed in Figures 21 and 22.

A similar trend was observed, the temperatures decayed in soil as the distance from the pile surface increased, at both depths, 80 and 400 mm (Figures 20 and 21). The inlet temperature for this pile was slightly higher than that of 2U-Pile, 51°C. At 80 mm depth, the temperature reached 41°C at the pile surface and decayed to 35.5, 30 and 24.5°C at distances of 30, 150, and 360 mm, respectively. At 400 mm depth, the temperature reached 48°C at the pile surface and reduced to 36, 32 and 28°C at distances of 30, 150, and 360 mm, respectively. These temperatures were reached in the three cycles and all the temperatures in all positions converged to the same temperatures ~ 23°C, during cooling, which signifies and confirms a recovery. As in 2U-Pile results,

the temperatures at 80 mm presented lowered readings than those at 400 mm depth (Figure 22).

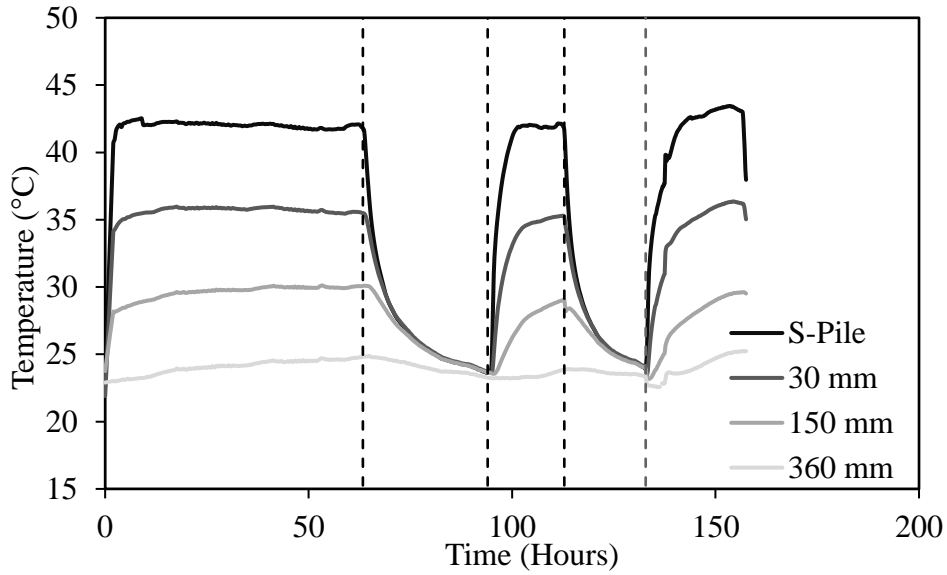


Figure 20. Temperature variation during S-Pile cycles at 80 mm depth

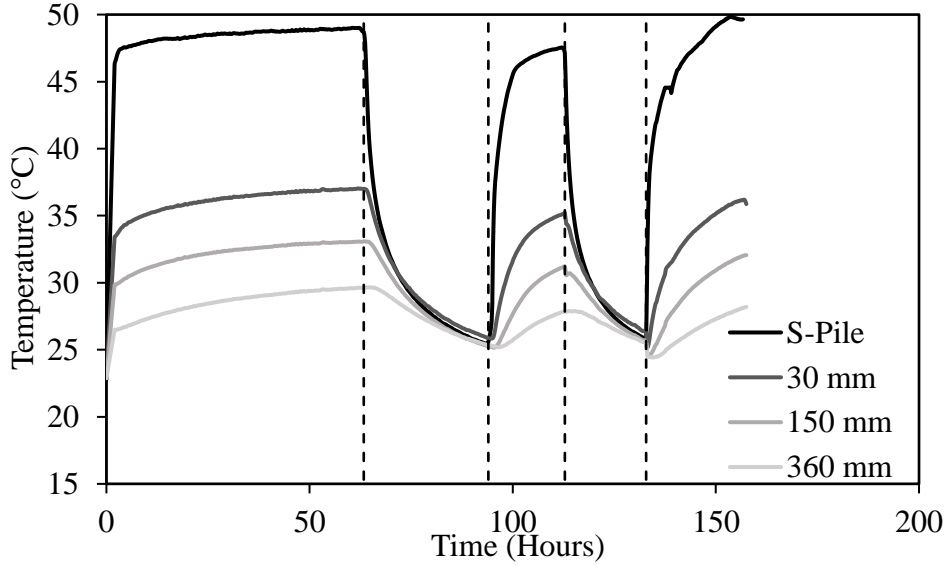


Figure 21. Temperature variation during S-Pile cycles at 400 mm depth

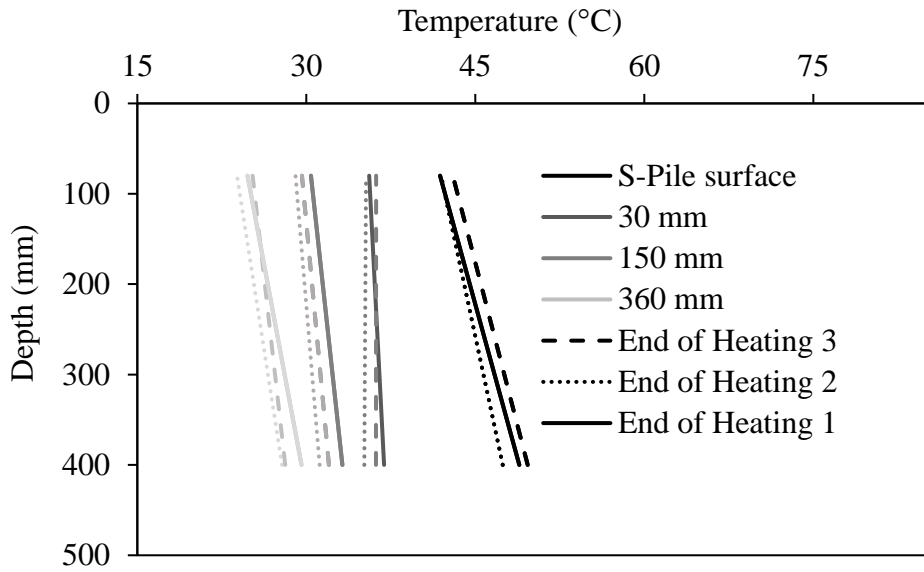


Figure 22. Temperature profiles at the end of heating phases for S-Pile

Due to defected thermocouple, the inlet temperature was only measured during the third cycle, thus the thermal exchange rate was calculated only for that cycle. As shown in Figure 24, like 2U-Pile results, the thermal exchange rate fluctuates around an average of 205 W/m.

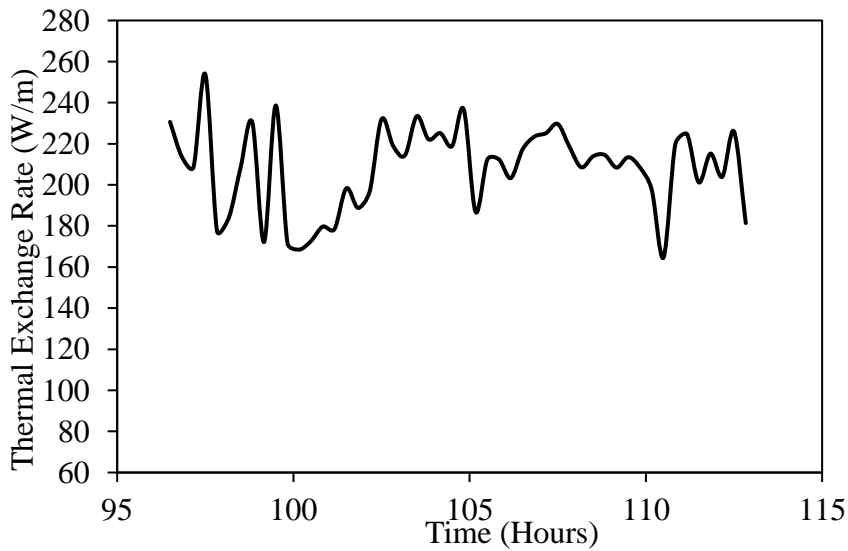


Figure 23. Thermal exchange rate around the S-Pile

### 3.3.4 Analysis

#### 3.3.4.1 Thermal Cycles Results:

Since the changes in the temperature profiles were relatively minimal between cycles, the results of the first cycle were used to compare the increase in temperature (relative to ambient temperature  $\Delta T = T - T_{\text{ambient}}$ ) at depths of 80 mm and 400 mm during heating (Figure 24).

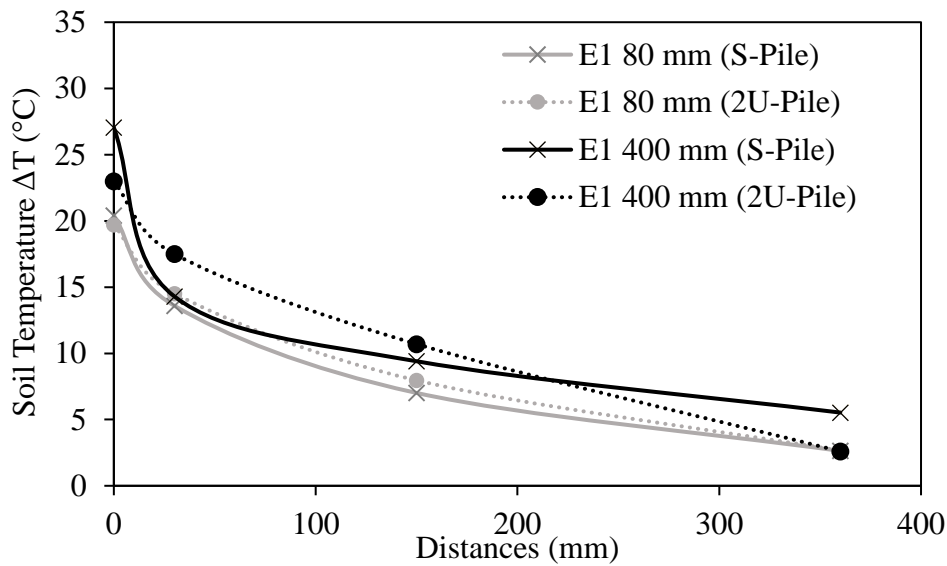


Figure 24. Soil temperature distribution along radial distance from the piles' surfaces

Results indicate that at a relatively shallow depth of 80 mm, the increase in the observed soil temperature is very similar in the two pile configurations (S and 2U). Both piles show similar temperature increments at the pile surface (19.6°C) and in the soil at all radial distances. This indicates that at shallow depths, the type of pipe configuration does not affect the heat exchange rate of the pile. At a depth of 400 mm, the increase in temperature was clearly larger at the surface of the S-Pile (27°C compared to 23°C). Despite this higher temperature, results on Figure 25 indicate that the soil temperature at 400 mm depth around the S-Pile decreased dramatically (drop of 13 °C at 30 mm) compared to a relatively modest decrease (5 °C) at 30 mm from the surface of the 2U-

Pile. This difference in  $\Delta T$  between the two piles becomes less significant at farther radial distances (180 mm and 360 mm). These results are interesting since they indicate that at a depth of 400 mm, the soil was able to absorb more heat near the 2U-Pile although the S-Pile configuration exhibited higher temperature along the pile itself. Additional testing needs to be done in the future to confirm and explain these observations.

Figure 25 shows the variation of the heat exchange rate with time for the two geothermal piles during the third heating cycle. The variations in the values were caused by the slight variation in the inlet/outlet temperatures with time. It is clear that the pile with the spiral tubing configuration exhibits a higher efficiency with an average thermal output of 205 W/m compared to 110 W/m for the 2U-Pile. Such results are in agreement with the thermal performance tests conducted by Luo et al. (2016).

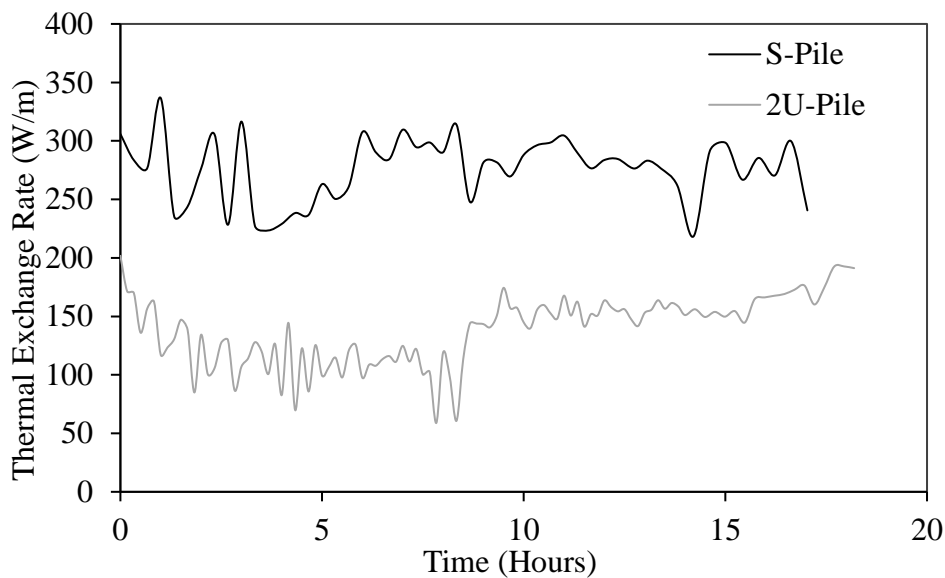


Figure 25. Variation of thermal exchange rate of the geothermal piles during heating

### 3.3.4.2 Uplift test results

The C-Pile wasn't subjected to thermal cycles, and it was pulled-out. In addition, the two geothermal piles were pulled out at the end of the cycles and the variation of the mobilized skin friction with vertical pile displacement are shown in Figure 26. The mobilized skin friction at any given displacement was calculated as the measured uplift force divided by the embedded surface area of the pile.

—

Equation 2. Mobilized skin friction (kPa).

The first difference is in the response at very small displacements (less than 0.3 mm) where the geothermal piles show a stiffer response when compared to the control pile. At these very small displacements, the piles that were subjected to cycles of heating and cooling showed mobilized skin friction values that were larger than those were witnessed in the control pile. It could be concluded that the heating cycles have affected the mechanical properties of the soil, resulting in an uplift mode of failure that is more 'brittle' than that observed in the control pile where the clay around the pile was not subjected to any heat exchange.

The second difference between the control pile and the energy piles is in the maximum observed mobilized skin friction at 3 mm pile head displacement, 2.5% of pile diameter. The control pile exhibited the highest mobilized skin friction (5.73 kPa) compared to that of the S-pile (5.2 kPa) and that of the 2U-pile (5.38 kPa). The reduction in skin friction as a result of 3 heating and cooling cycles could be calculated as 9.2% and 6.1% for the S-Pile and the 2U-Pile, respectively. These reductions in skin friction are observed despite the fact that the average undrained shear strength in the

clay at the locations of the energy piles was 11% and 18% higher than that of the clay at the location of the control tests. These results are important since they indicate that although the reduction in skin friction due to heating and cooling seems to be relatively small (less than 10%), the reduction in the adhesion factor (  $\alpha$  ) which is defined as the ratio of the mobilized skin friction to the undrained shear strength of the clay could be more significant.

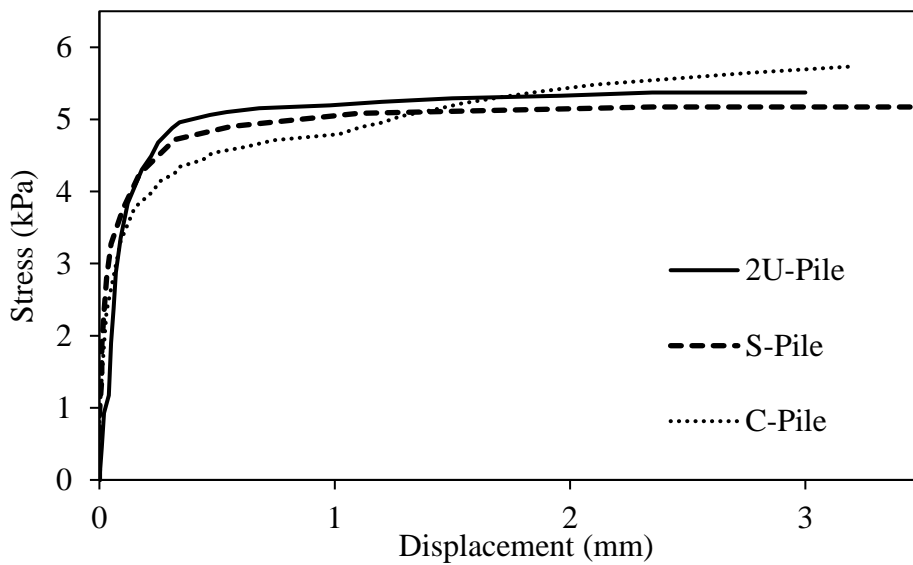


Figure 26. The three piles uplift test results

Given the initial average undrained shear strength values for the three piles, the empirical adhesion factor (  $\alpha$  ) was calculated for each pile using the maximum mobilized skin friction observed in each test such that:

$$\alpha = \frac{f_{skin}}{S_{u,average}}$$

Equation 3. Empirical adhesion factor.

Where  $f_{skin}$  is the ultimate skin friction (kPa) and  $S_{u,average}$  is the average undrained shear strength (kPa). The calculated  $\alpha$ -values are 0.43, 0.35 and 0.34 for the control pile, the S-pile, and the 2U-Pile, respectively. The percent decrease in the

adhesion factors in the S and 2U piles compared to the control pile could be calculated as 18.27% and 20.35%, respectively. These decreases in  $\tau$  are significant and may have to be accounted for in the design of energy piles that are embedded in slightly over consolidated clay, under tension/uplift loads. Note that these reductions in adhesion between the pile and the soil were observed after very limited cycles of heating and cooling (3 heating and 2 cooling). The reductions could be more significant for identical piles that are subjected to additional cycles, as will be the case in real applications involving energy piles.



## CHAPTER IV

### EXPERIMENTAL MODEL II

#### 4.1 Overview

The first experimental model focused on comparing the pile frictional capacity of geothermal piles subjected to heating cycles with control pile, in addition to the efficiencies of two tubing configuration.

For the second experimental model, the same soil and piles specifications were used. However, the piles were subjected to load to mimic real life situation in which the piles will have a working load. The load used was only tension to restrict the capacity of the pile to its skin friction. The three piles in this section were exposed to a working load tension of 300 N, 30% of the ultimate capacity, for three days before the initiation of thermal cycles and it was maintained during the cycles. The ultimate capacity of the pile in uplift was estimated to be approximately 1000 N based on a previous experimental testing program that was conducted with the same experimental setup. The first pile (C-Pile) was subjected to tension load only. Whereas the other two geothermal piles were subjected to 3 cycles of heating and cooling identical to that cycles in the first experimental model. The S-Pile was exposed to addition cycles at the end of Cooling 3. This procedure enabled us to compare the results of the previous setup subjected to cycles only with the results of the piles subjected to same cycles but with tension. In addition, we were able to study the effect of additional cycles on the friction compared to piles subjected to three cycles only.

## **4.2 Testing Procedure**

The bed preparation and piles implementation were identical to the procedures taken in experimental model 1. During cycles, the temperature variations were censored using thermocouples distributed as shown in Figure 15, and the piles head displacement was monitored using LVDT. The inlet temperature for both piles was constant at 48 °C.

The test sequence was divided into three parts, each discussing the procedure of one pile.

### **4.2.1 Step 1**

The testing started with the control pile to ensure that the heat from the adjacent thermal piles did not affect it. After placing the LC, LVDT and gauges, the 300 N were added gradually and kept for 72 hrs. Then an uplift test was conducted by adding loads over the 300 N using the same system described in section 3.2 and shown in Figure 16.

### **4.2.2 Step 2**

Similarly, testing of 2U-Pile was initiated with sustained loading at 30% of the ultimate capacity for three days using a simple load-controlled system. After sustaining the working load for three days, the 2U-Pile was subjected to three thermal cycles. The first cycle consisted of 3-days heating and 1-day recovery while the subsequent two cycles consisted of 1-day heating followed by 1-day recovery. At the end of the cycles, the pile was pulled-out at a “fast” rate to estimate its undrained ultimate capacity.

### **4.2.3 Step 3**

The same procedure was adopted for the S-Pile with additional 6 thermal cycles of 1-day heating followed by 1-day recovery. Similarly, an uplift test was carried out for the S-Pile after the completion of the thermal cycling phase.

## **4.3 Results**

### **4.3.1 Working Load**

The three piles were initially subjected to a 300 N tension force for three days. Upon the application of the sustained load, an immediate upward movement was measured. This movement slightly increased with time and became constant at around 0.22 mm, 0.20 mm, and 0.16 mm for the C-Pile, 2U-Pile and S-Pile, respectively.

### **4.3.2 Temperature results during cycles**

#### **4.3.2.1 2U-Pile cycles**

During cycles, displacement, load and temperature were monitored. The variation of the temperature with time at the surface of the pile and within the soil is presented in Figure 28 and 29, at 80 and 400 mm depth, respectively. The temperature of the pile increased during the first 7 hours of heating reaching maximum values of 40.5°C for the 2U-Pile. As expected, the temperature in the soil was lower as we move away from the pile surface. At the end of heating the net increase in the soil temperature (compared to ambient) was 10°C at a distance of 80 mm and 3°C at 360 mm for the 2U-Pile. In addition, Figure 29 shows same phenomena of an increase in temperature with depth as observed in E1. It is worth noting that due to technical problems with the water pump, sudden changes in temperature occurred in the first heating cycle for the 2U Pile.

This incident did not influence the results as the target temperatures were reached and maintained beyond that point.

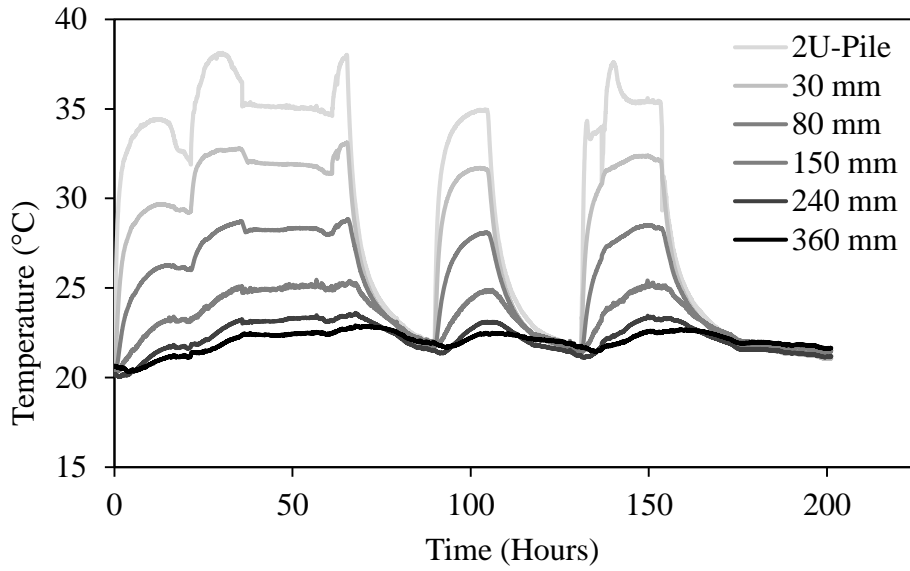


Figure 27. Temperature variation during 2U-Pile cycles at 80 mm depth

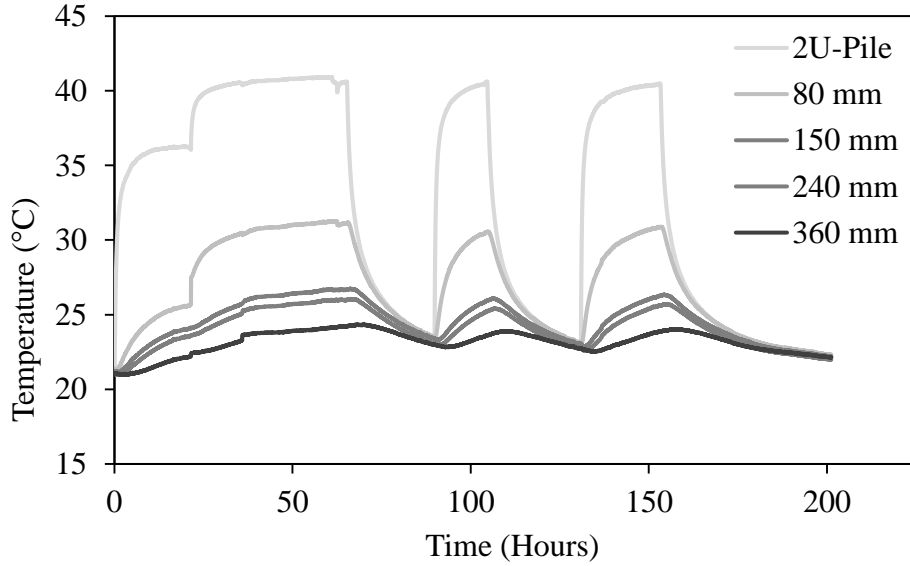


Figure 28. Temperature variation during 2U-Pile cycles at 400 mm depth

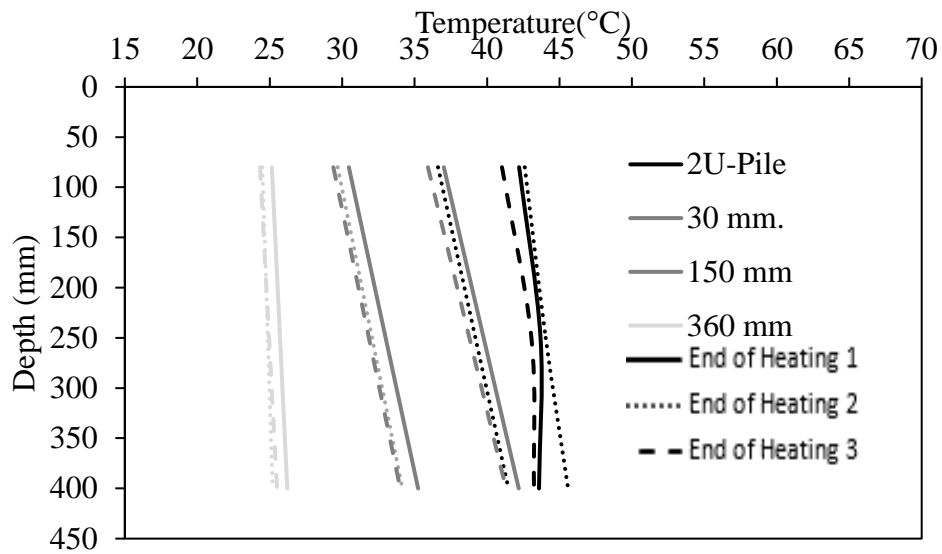


Figure 29. Temperature profiles at the end of heating phases for 2U-Pile

The thermal exchange rate was estimated to evaluate the thermal efficiency of the 2U-Pile at a constant temperature (Figure 30). The drop in the rate during the first 20 hours of the first cycles is due to the technical problem in the water bath mentioned earlier. However, during the second part of the first cycle and consequent cycles, the rate varies under a small range with an average of 190 W/m.

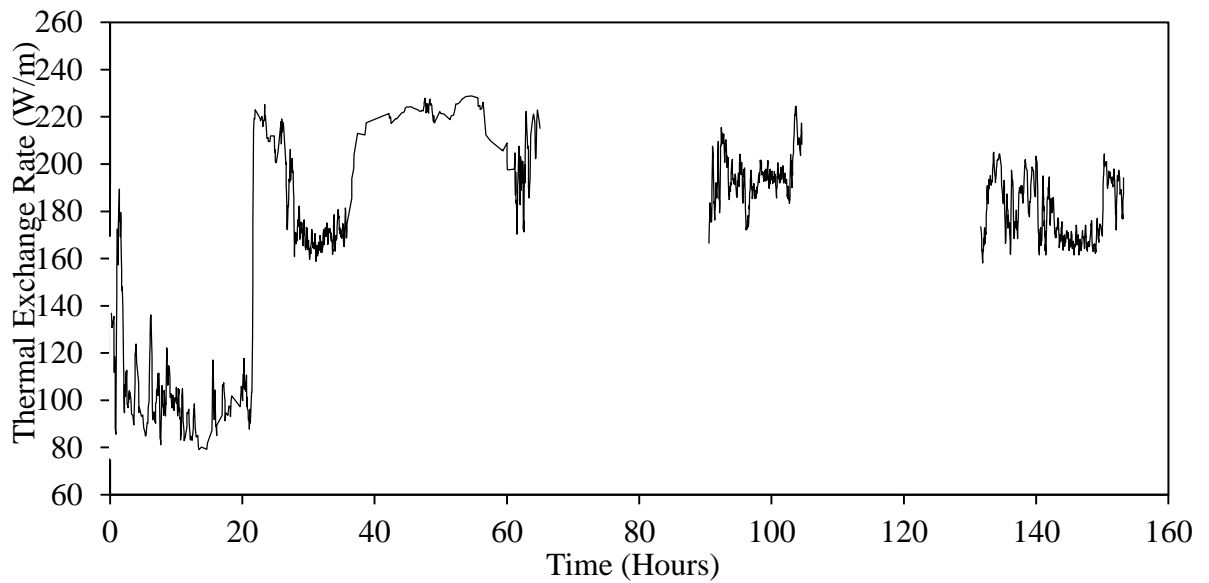


Figure 30. Thermal exchange rate around 2U-Pile during the three cycles

#### 4.3.2.2 S-Pile cycles

The S-Pile was subjected to nine thermal cycles compared to 3 cycles for the 2U-Pile. The temperature of the pile increased during the first 7 hours of the first three heating cycles reaching maximum values of 42°C compared to 40.5 °C for 2U-Pile at 400 mm depth. During the additional eight cycles, the temperature across the soil showed analogous values. Similarly, during recovery, the minimum reached temperatures were similar at 80 mm and 400 mm depth as shown in Figures 31 and 32, respectively.

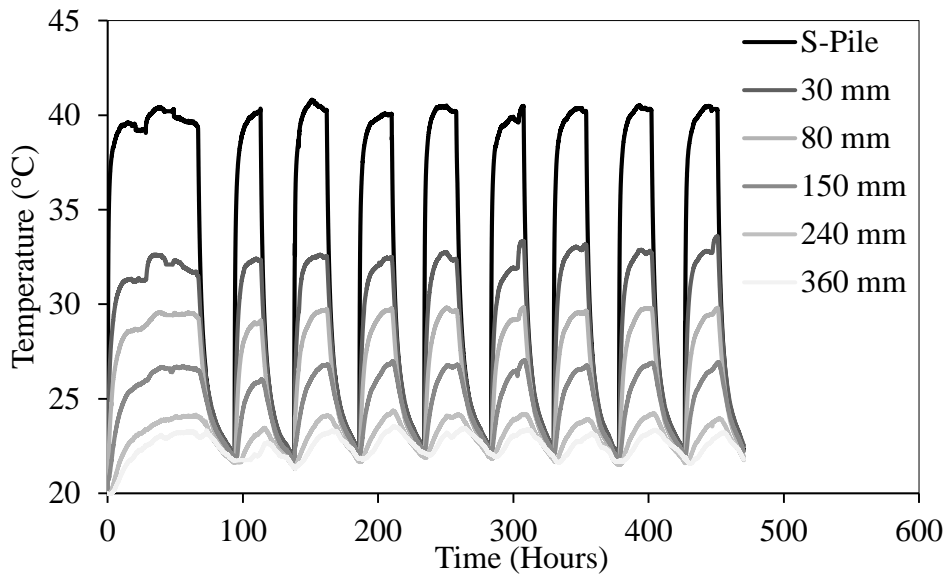


Figure 31. Temperature variation during S-Pile cycles at 80 mm depth

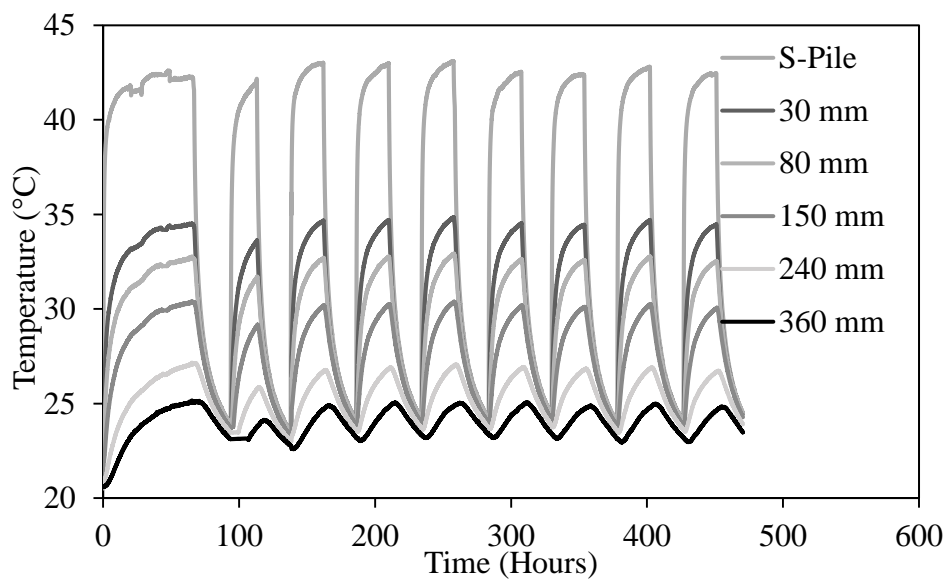


Figure 32. Temperature variation during S-Pile cycles at 400 mm depth

The same trend of temperature distribution with depth was observed as 2U-Pile in E2 and both piles in E1.

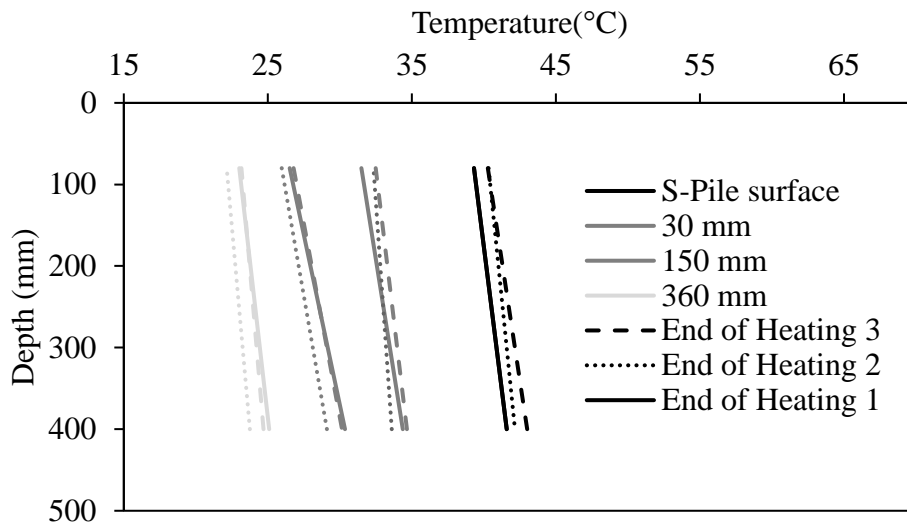


Figure 33. Temperature profiles at the end of heating phases for S-Pile

To better analyze the thermal efficiency of the S-configuration, the thermal exchange rate was evaluated using the difference between inlet and outlet temperatures using same equation (1). The variation in the rate is shown in Figure 34 through the nine heating phases. It was noticed that the first two cycles (250 and 288 W/m) had variable rate and significantly higher values than the rate during the following cycles ~185 W/m. The lower rate during cycle one might be due to the fluctuations in the initial temperature values before reaching a steady value after 7 hours. Starting with the Fourth cycle, the thermal exchange rate reached a steady state with an average value of 184 W/m (Figure 35).



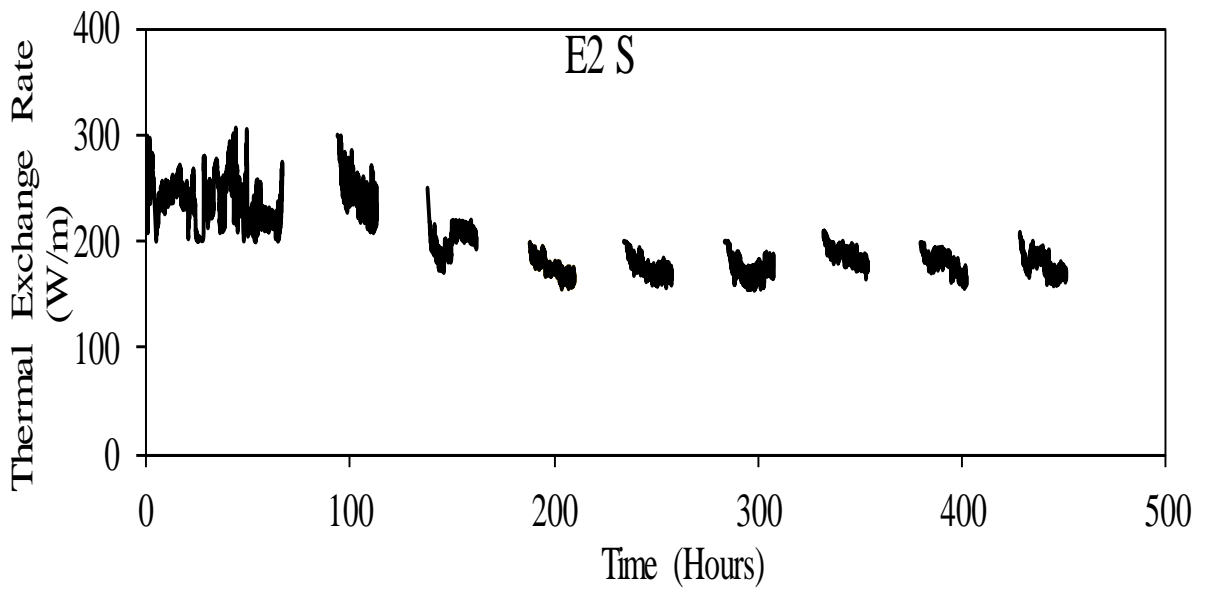


Figure 34. Thermal exchange rate around S-pile

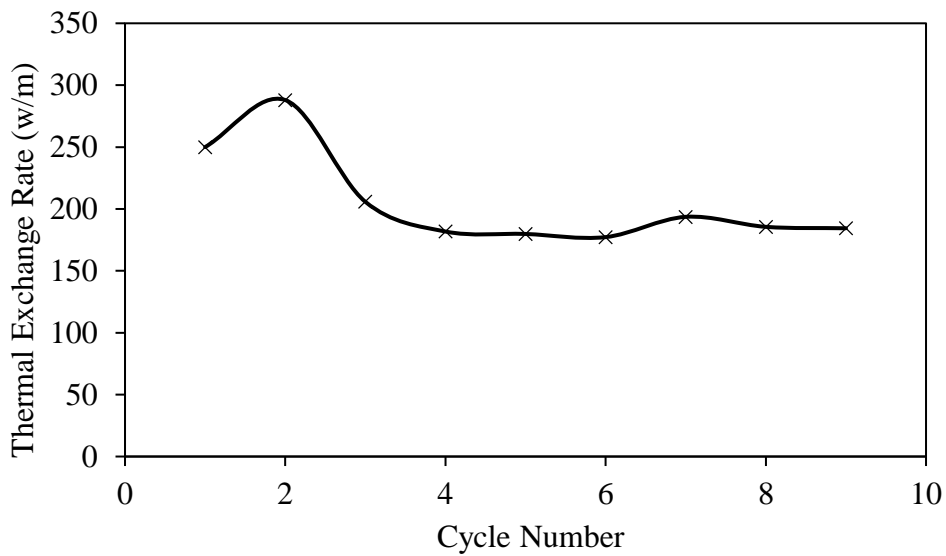


Figure 35. Thermal exchange rate during cycles

#### 4.3.3 Head displacement and load results during cycles

Both displacement and load showed a variation in their values with respect to the change in temperature as the cycles alternated between heating and recovery. The three piles were initially subjected to a 300 N tension force for three days. For the

energy piles, thermal cycles were initiated in the presence of the sustained load. The variation of the pile heads displacements with temperature are presented in Figure 37 and 39, for 2U-Pile and S-Pile, respectively. Results indicated that the pile heads moved upward during heating with partial recovery of deformation measured during cooling. The head of the pile retained a cumulative plastic movement, which increased in value with thermal cycles. This ratcheting effect was also observed by Ng. et al (2014) for the pile placed in slightly overconsolidated clay but with a downward trend due to the applied compression load. The final irreversible pile displacement was 0.6 mm for the 2U-Pile and 1.5 mm for the S-Pile. It is interesting to note that the S-Pile exhibited larger displacement than 2U-Pile during the initial three identical thermal cycles. This may be due to the higher heat transfer efficiency of the S-configuration which induced higher temperatures at the soil/pile interface and within the soil. In addition to the pile head displacement, a variation in the load read by the LC was witnessed, an average of -16 N during heating and +16 N during cooling from the sustained load 300 N (Figures 36 and 38).

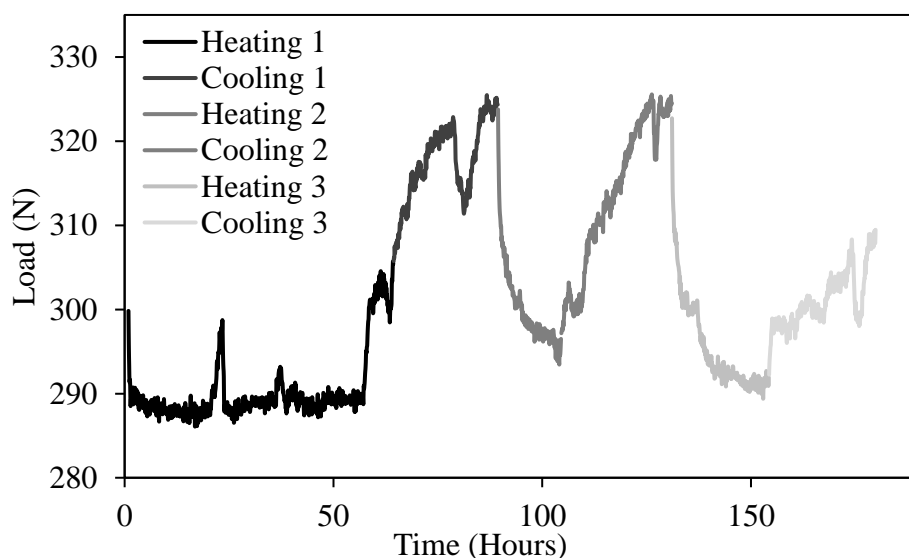


Figure 36. Variation in load during 2U-Pile cycles

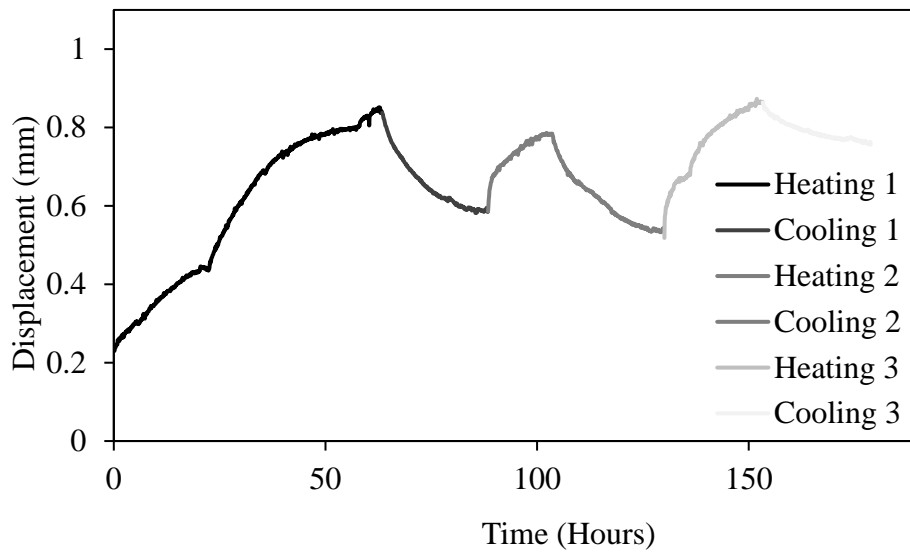


Figure 37. Variation in pile head displacement during 2U-Pile cycles

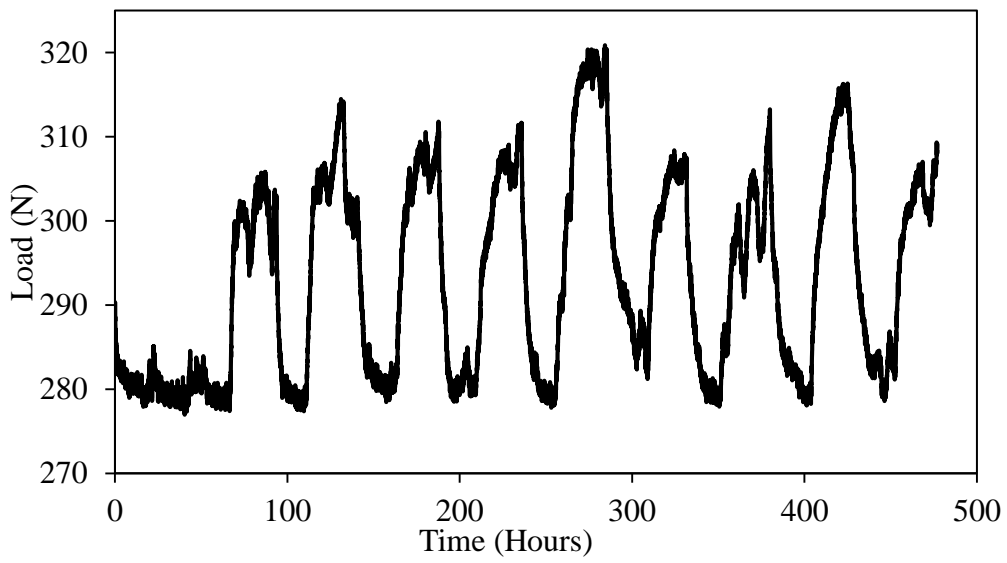


Figure 38. Variation in load during S-Pile cycles

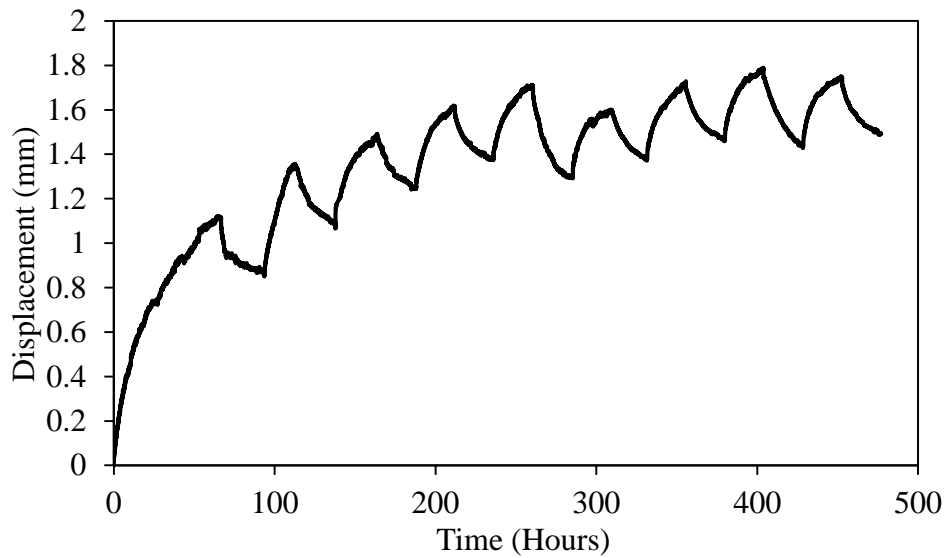


Figure 39. Variation in pile head displacement during S-Pile cycles

#### 4.3.4 Analysis

##### 4.3.4.1 Thermal cycles results

Similar temperature increases (compared to ambient) were noticed for the soil around the S-Pile and 2U-Pile. But, the soil around the S-Pile showed higher values at 400 mm depth, 12.5 and 8.5°C, compared to 11 and 4.6°C at 30 mm and 360 mm, as shown in Figure 40. Whereas at 80 mm depth, the soil around both had almost same increase at different radial distances from the pile surface.

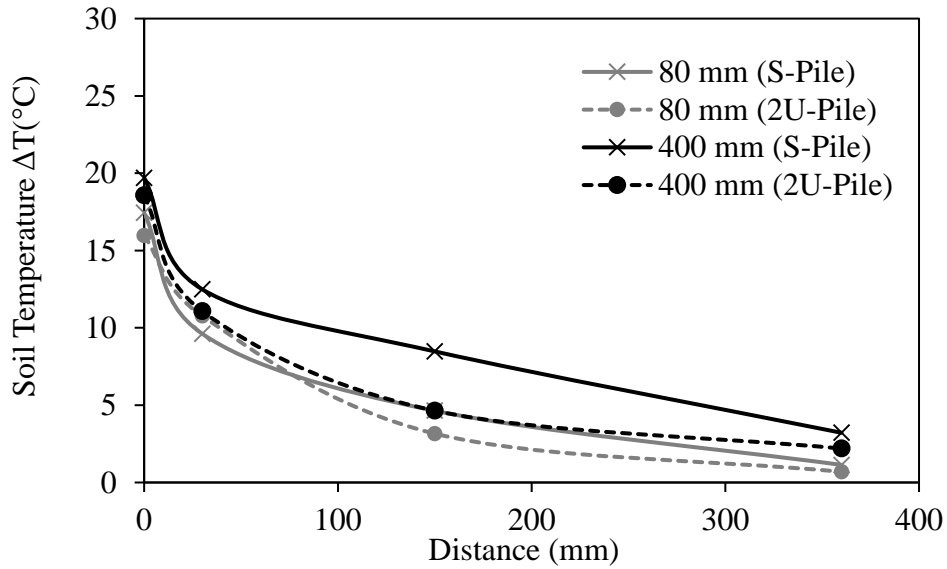


Figure 40. Soil temperature distribution along radial distance from the piles' surfaces

As shown in Figures 30 and 34, the thermal exchange was estimated for both geothermal piles to check their thermal efficiency. And by taking values for 1 cycle for each pile, the second cycle since it is comparable. The average thermal heat exchange is 240 W/m and 190 W/m for the S-Pile and 2U-Pile, respectively. These results confirm that the S-Pile is thermally more efficient than 2U by having 26 % higher rate (Figure 41).

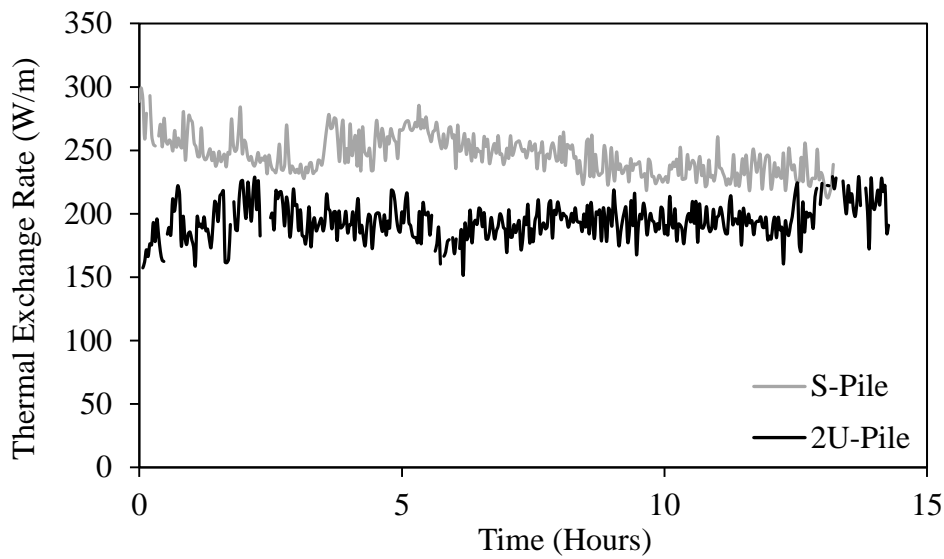


Figure 41. The thermal exchange of the two piles during heating cycles

#### 4.3.4.2 Head Displacement

To investigate the possible contribution of free thermal expansion to the observed top pile displacements, the free thermal expansion was calculated and plotted in Figures 42 and 43, assuming that the pile toe is fixed and ignoring the side resistance. This expansion is assumed elastic, in which it expands during heating and contract back to its original form during recovery. Results show that the free thermal expansion constituted a small part of the observed pile displacement which accounted to more than 5 to 8 times the calculated thermal expansion for the 2U-Pile and S-Pile, respectively. The observed displacements that are in excess of the estimated thermal expansion are attributed to a phenomenon occurring within/at the soil/pile interface zone as a result of thermal cycling. This phenomenon resulted in additional creep that increased with the number of heating cycles. It is worth noting that the partial displacement recovery that was observed in the cooling part of each cycle was accompanied by slight increases in the loads measured as indicated in Figures 36 and 38. This minor increase in the load

during cooling could be attributed to contraction in the pile material or to a thermally-triggered “downdrag” where the clay around the pile pulls the pile downwards.

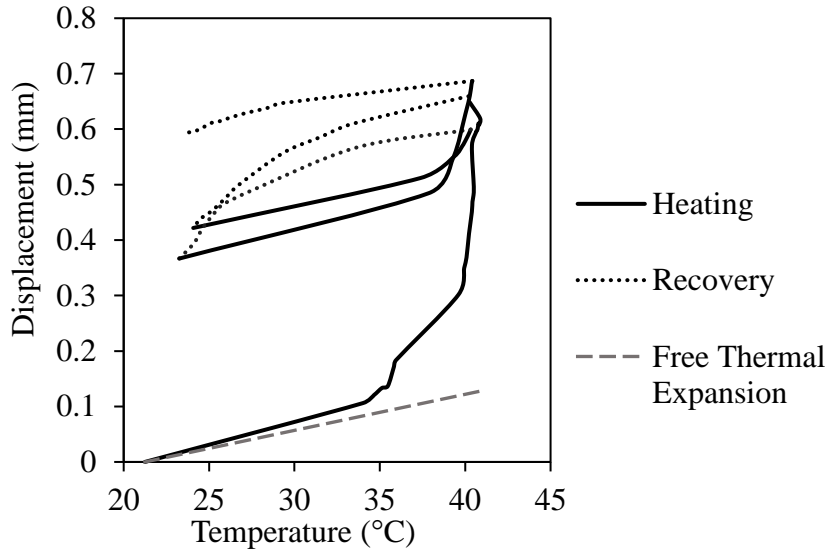


Figure 42. Head displacement as a function of temperature for 2U-Pile

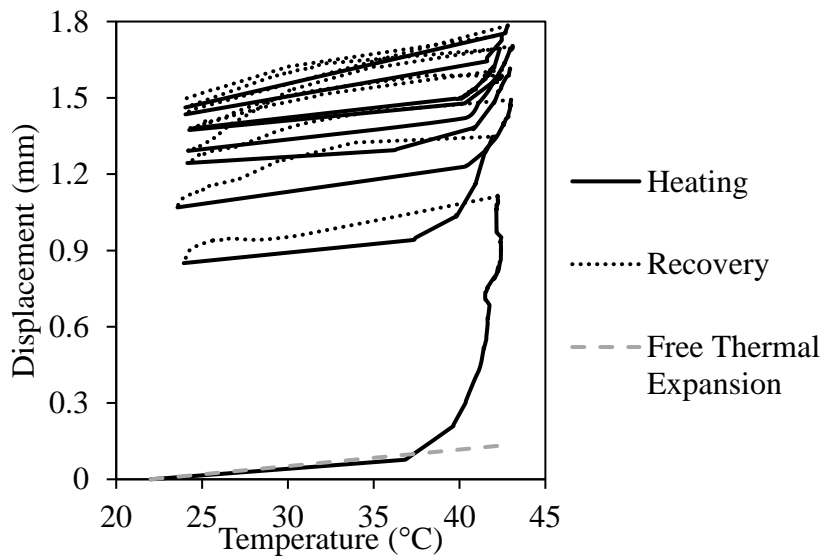


Figure 43. Head displacement as a function of temperature for S-Pile

Figures 42 and 43 show an initial plastic deformation as a result for the first heating cycle that is relatively large compared to the consequential cycles. Heating in the first cycle lasted (~67 Hours) which explains the high displacements compared to ~

22 Hours in the following cycles. On the other hand, a decrease in the supplementary plastic deformation was witnessed as the number of the cycles increased in both piles.

#### 4.3.4.3 Uplift test results

At the end of the thermal cycles, the piles were pulled out to measure their mobilized skin friction and examine any change due to heating. The results of the pullout tests are presented in Figure 44. The mobilized skin friction was calculated using Equation 2. Results point to some differences in the response of the geothermal piles. The S-Pile presented an initially stiffer response compared to the 2U pile and the Control pile but failed in a more brittle manner compared to the other two piles. At failure, the geothermal piles exhibited a slight reduction in skin friction compared to the control pile. The maximum mobilized skin friction was 5.7 kPa, 5.46 kPa (4.2% reduction), and 5.2 kPa (8.74% reduction) for the C-Pile, 2U-Pile, and S-Pile respectively. The adhesion factor ( $\alpha$ ) was calculated using Equation 3. It also exhibited reduction upon heating/cooling with the reduction estimated as 11.52% for the 2U-Pile and 14.45 % for the S-Pile. This suggests that using the piles as energy sinks may affect their ultimate capacity. The negative effect seems to be greater for the S-Pile, which was subjected to additional heating cycles indicating that the response of the energy piles at ultimate may be related to the number of thermal cycles they are subjected to.



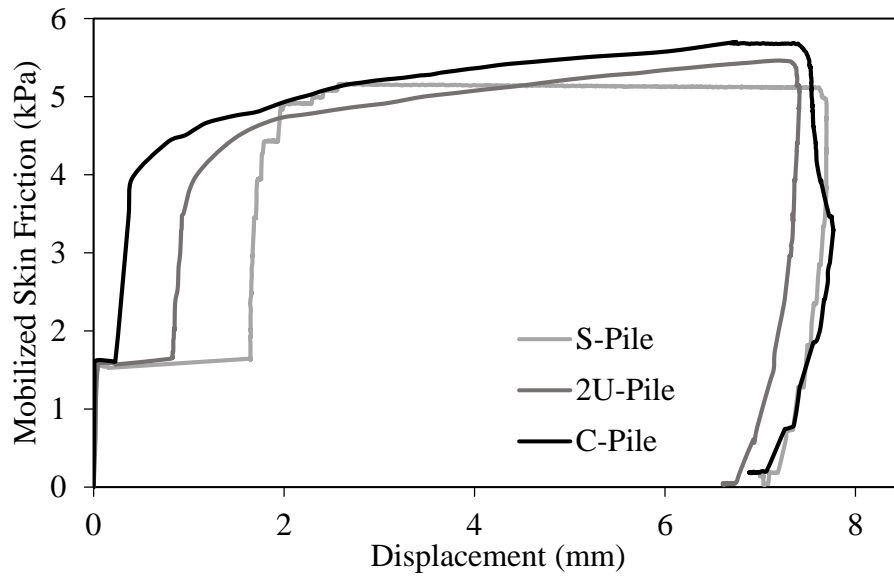


Figure 44. The three piles uplift test results

## CHAPTER V

### RESULTS ANALYSIS

Both experiments underwent the same procedures except adding a sustained load for the pile heads during the second experimental setup and having additional cycles during the S-Pile testing. The experimental tests are further compared and analyzed through this chapter.

#### **5.1 Thermal Response**

The energy piles were subjected to inlet temperature of 48 °C except the S-Pile of the first setup, the temperature was slightly higher, 51 °C. The thermal response of the energy piles is best examined by comparing the difference in temperature in soil (Figure 45). The temperature difference shows a consistent trend through soil in the graphs. The graphs show slightly higher values during E1 at 150 mm distance. This might be due to a small difference in the characteristics of the soil due to experimental errors. However, graphs in Figure 45 (a) and (b) show somewhat lower values at depth 80 mm than that in Figure 45 (c) and (d) at 400 mm depth. Despite the difference in the response at close distances, at 80 mm depth, all the curves converged towards the same increment  $\sim 2^{\circ}\text{C}$ . Whereas at 400 mm depth, the S-Pile showed higher values at further distances from the pile surface  $\sim 4^{\circ}\text{C}$  compared to  $\sim 2^{\circ}\text{C}$  from the 2U-Pile at 360 mm distance.

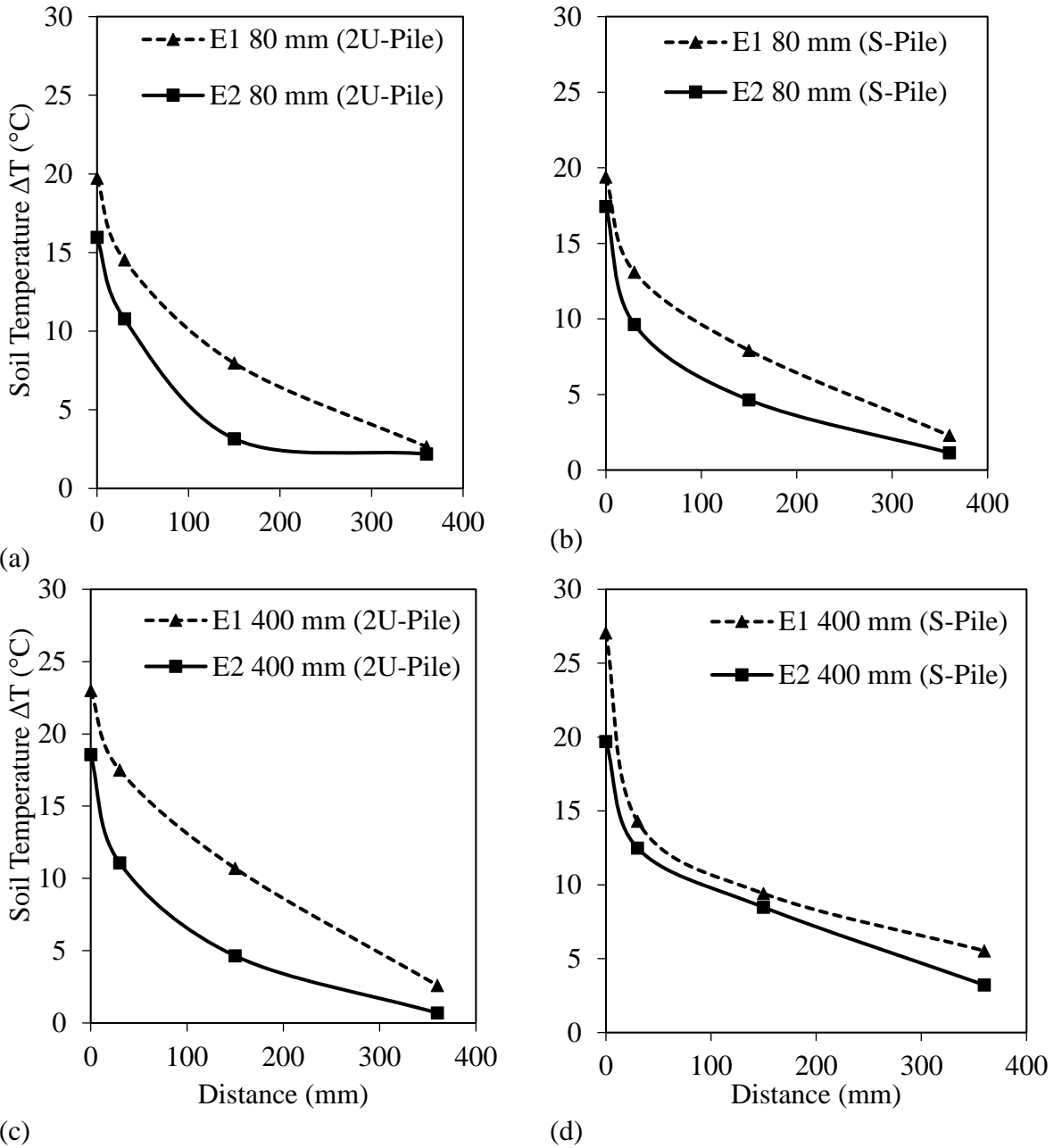


Figure 45. Comparison of the temperature distribution in soil around pile for during heating in E1 and E2 at depth 80 mm for (a) 2U-Pile and (b) S-Pile and at 400 mm for (c) 2U-Pile and (d) S-Pile

To have a better comparison for the efficiency of the two configurations, the thermal exchange of the two experimental tests were compared in Figures 46 and 47.

Only the third cycle was used to compare the rate, since this is the only available cycle for S-Pile in E1. Figure 47 shows the rate for S-Pile with average of 205 and 240 W/m

during E1 and E2, respectively. Whereas the rate for 2U-Pile had an average of 110 and 190 W/m, for E1 and E2, respectively (Figure 48). These plots show a coherent and consistent performance. In addition, it confirms the higher efficiency of S-Pile configuration by having nearly double the thermal rate exchange of 2U-Pile configuration.

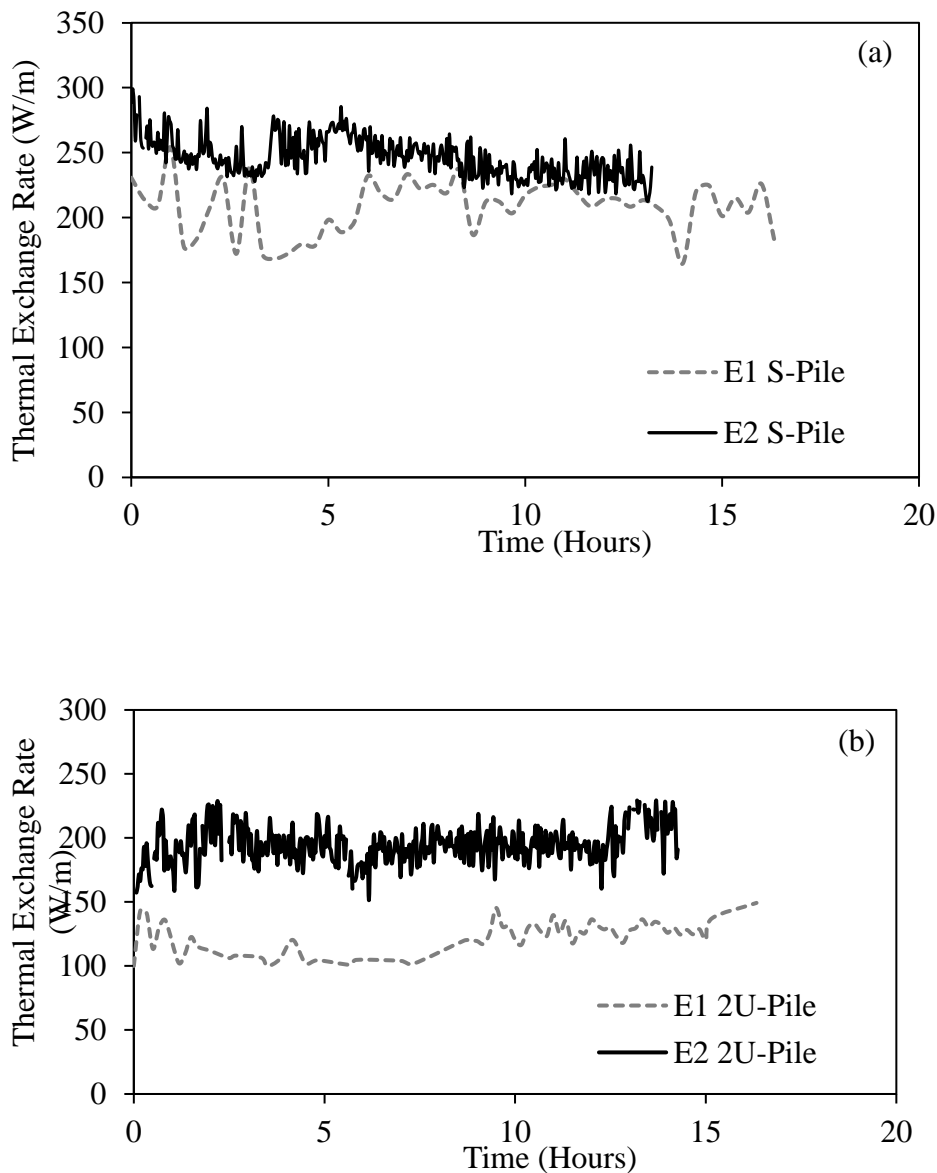


Figure 46. Comparison of the thermal exchange of the energy piles in the two experimental tests for (a) S-Piles and (b) 2U-Piles

## 5.2 Mechanical Response

The mechanical capacity of the piles, particularly the mobilized skin friction, was tested by uplift tests. Using the undrained shear strength at the position of each tested pile, the adhesion factor was evaluated to better compare the thermal effect of the cycles on the pile's capacity.

Table 2. Uplift test result during E1 and E2

Pile	Cu Value (kPa)	Skin Friction (kPa)	Adhesion Factor	Decrease in Adhesion (%)
Experimental Model 1				
C-Pile	13.31	5.73	0.43	-
2U-Pile	15.68	5.38	0.34	20.3
S-Pile	14.73	5.2	0.35	18
Experimental Model 2				
C-Pile	17.71	5.7	0.32	-
2U-Pile	19.17	5.46	0.28	11.52
S-Pile	18.86	5.2	0.28	14.33

Table 2 summarizes the attained mobilized skin friction for each tested pile and its corresponding adhesion factor. The decrease in the adhesion factor for the energy piles was calculated compared to that of the control pile of each experimental model. Both experiments witnessed decrease in the adhesion with respect to the control piles. But C-Pile in E1 had a higher adhesion value than that in E2 despite the fact that, the undrained shear strength at C-Pile position is higher for E2 than for E1. In addition, the energy piles had lower values as well, during E2 compared to E1, this decrease can be contributed to the presence of sustained load during the second setup. This load resulted in a upward displacement during the first three days, which may weakened the soil/pile

interface. The preloaded piles in E2 tended to fail at lower loads since the uplift test in E1 was done in a fully undrained system. Whereas the uplift during E2 was done gradually, and 30 % load of the total load was already applied for a long duration which permitted a drained behavior. While only the other 70 % of the load was applied during the uplift in an undrained manner.

### 5.3 Pile head displacement during cycles

Pile head displacement was not read in experimental model 1, but readings were available for experimental model 2. Since the S-Pile was subjected to 9 consecutive cycles, its displacements were used to analyze its behavior. Figure 48 shows heave of the S-Pile head. This displacement increased during heating cycles and decreased during cooling. But this decrease was partial recovery, indicating a plastic displacement.

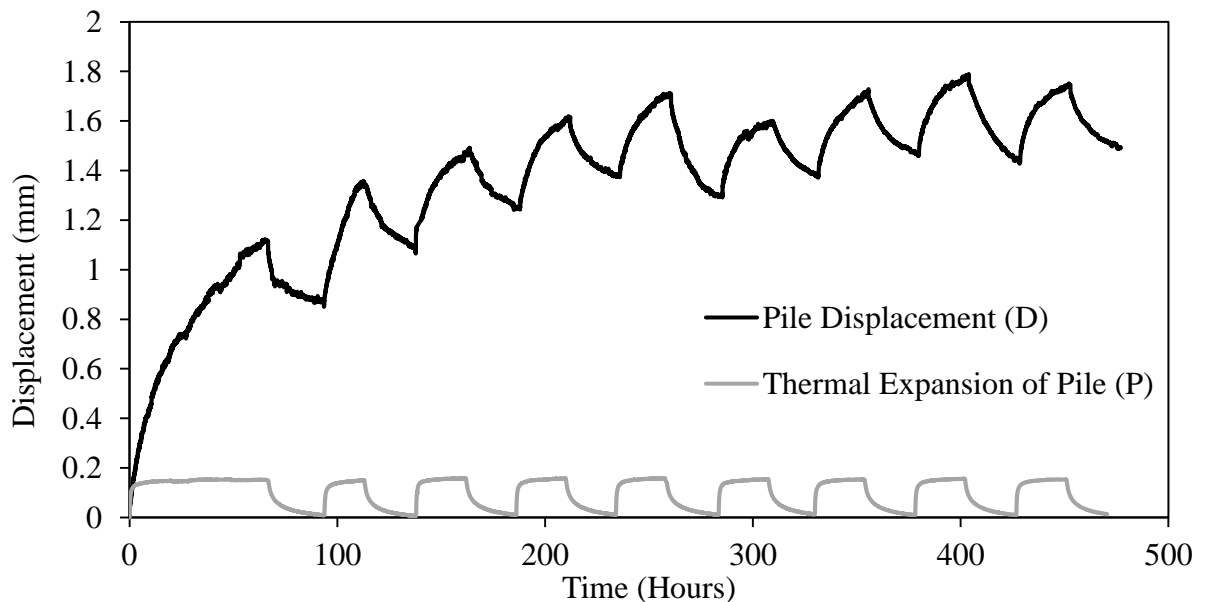


Figure 47. Pile head displacement and thermal expansion of the pile during cycle of S-Pile

The maximum reached displacement during each heating phase and the maximum endured plastic deformation at the end of each recovery phase are plotted in Figures 48 (a) and (b), correspondingly.

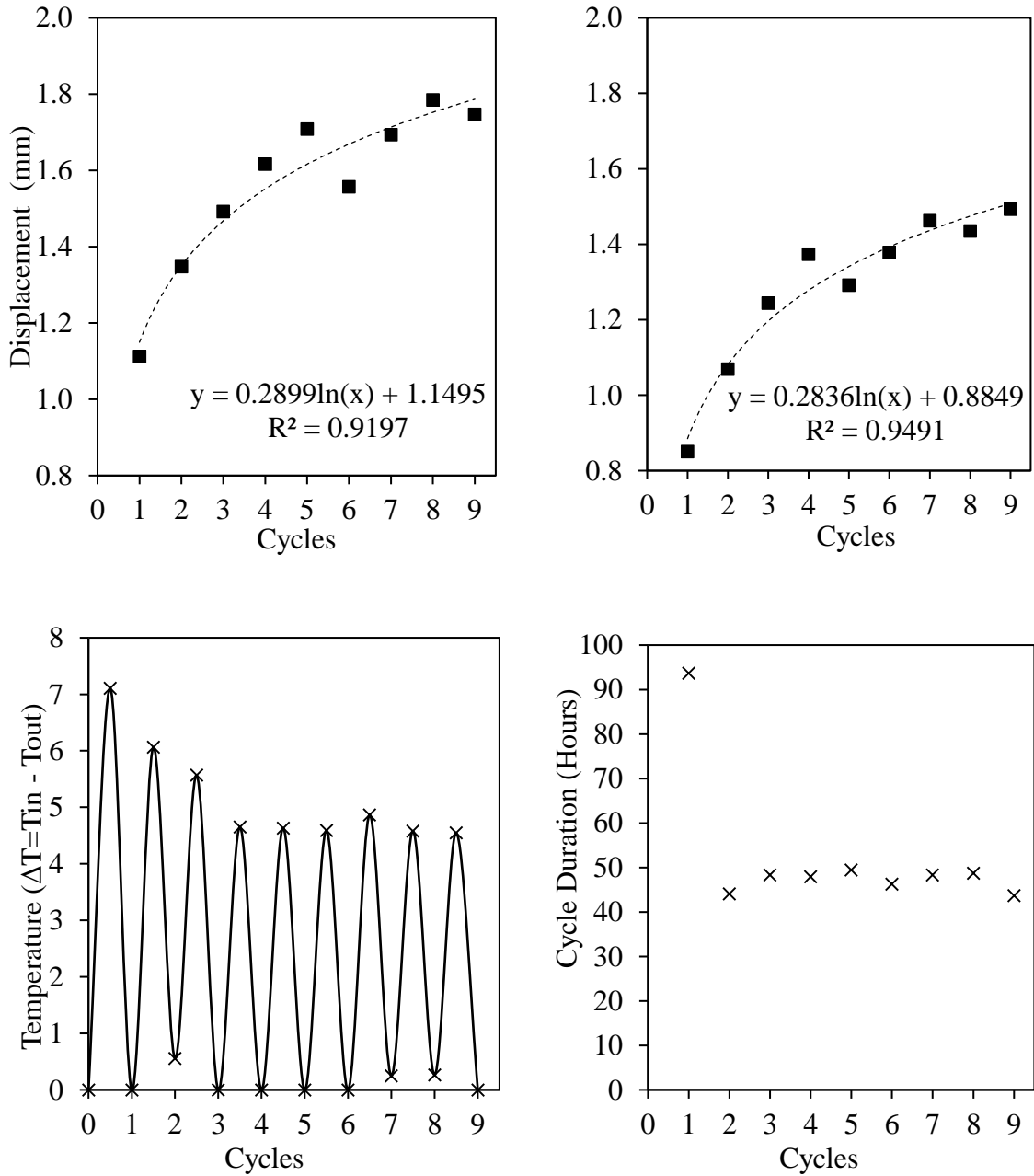


Figure 48. S-Pile cycles results (a) total pile head displacement during heating phase (b) total plastic deformation at the end of each recovery phase (c) maximum reached temperature difference during cycles and (d) duration of each cycle

Figure 48 (a) presents the total deformation at the end of each heating phase. This shows that under uniform cyclic thermal loading, upward movement of the pile increased gradually but eventually stabilized. Whereas Figure 48 (b) includes the total plastic deformation at the end of each cycle, which shows a same pattern as in the total displacement.

Many factors may affect the measurement of displacement, of which are the temperature level, and the duration of heating phase. Temperatures adopted in this research fall in the range adopted in the literature, however the durations vary depending on the region the energy piles are being implemented. So, quantifying the additional displacement during each cycle and dividing it with the duration of that cycle gives the graph plot shown in Figure 49. The data shows a decay in the plastic deformation with the increase in the number of cycles that can be modeled as a logarithmic function to predict these displacements. These data are not sufficient but shows that there is a trend in the behavior that with further studies can be predicted.

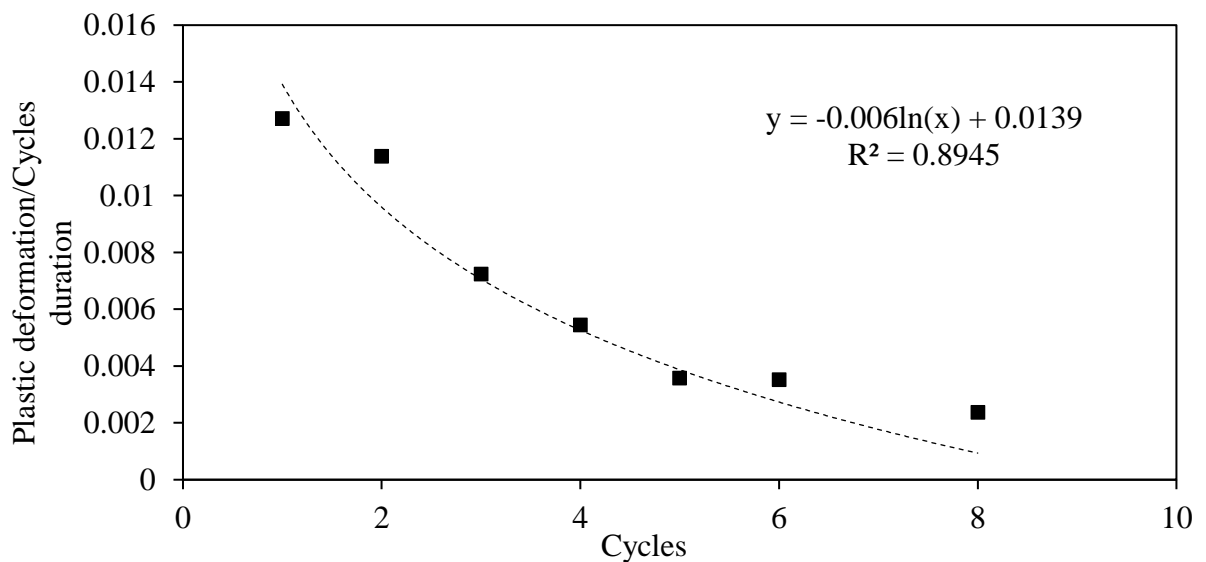


Figure 49. Variation of plastic displacement per unit time at the end of each cycle



Thermal expansion of the pile shown in Figure 47 presents part of the deformation that recovered. And to further comprehend the displacement, the difference between the total maximum pile head displacement during heating and the plastic deformation that remains during recovery was calculated to get the elastic deformation occurred for each cycle. This elastic deformation is presented in Figure 50 and compared to the piles thermal expansion. It is clear that the total recovered displacement is more than that of the expansion of the pile.

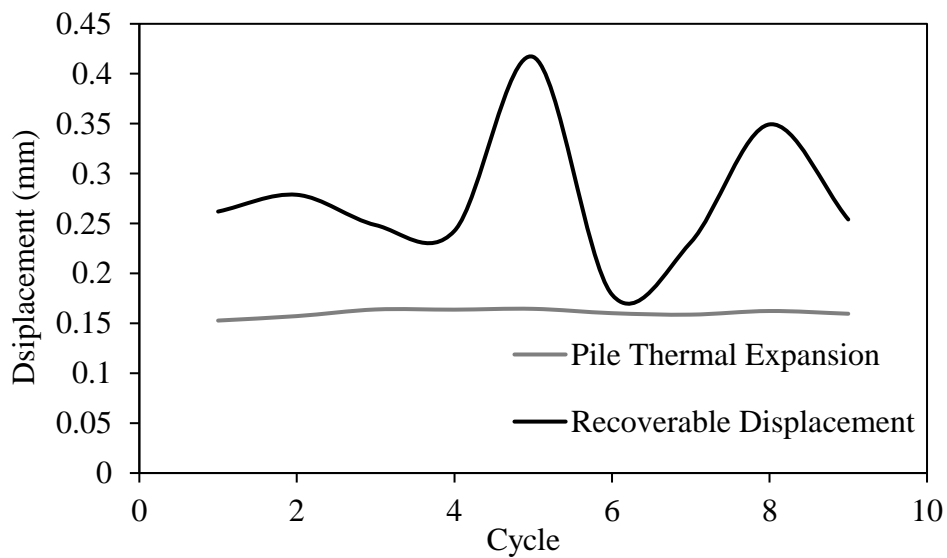


Figure 50. Recovered pile head displacement and thermal pile expansion

The difference in the displacement presented in Figure 50 confirms the contribution of the adjacent soil in the movement of the pile, which indicate a change in the capacity of that soil.

These data show the importance of understanding the response of the soil/pile interface under thermal loading.

## CHAPTER VI

### FINITE ELEMENT MODEL

To further understand the thermal behavior of soil and pile during cycles, a numerical analysis was conducted using finite element code Plaxis 2D Thermal. The finite element code PLAXIS 2D is well known for its capability for a fully coupled analysis involving thermo-hydro-mechanical processes.

Two simulations (mechanical loading only, and thermo-hydro-mechanical coupling) were conducted using the results obtained from the experimental models to validate the adopted FE model. The term of *validation* is defined in the context of numerical analysis as the process of testing software at the end of the software development process to evaluate its performance, assess its accuracy and correct operation by an individual and on specified hardware (Potts & Zdravković, 2001<sup>28</sup>). In this section, the existing validation procedures for the development of THM coupled facilities in the commonly used FE programs are summarized.

#### **6.1 Model Parameters:**

##### **6.1.1 Geometry:**

An axisymmetric finite element analysis was adopted to study the response of the energy piles. The dimensions of the model were identical to the experimental setup as shown in Figure 51. The soil consisted of 0.9 m layer of saturated soft clay and 0.1 m of sand. Interface was added at the soil-pile interface on the side and the bottom of the pile.

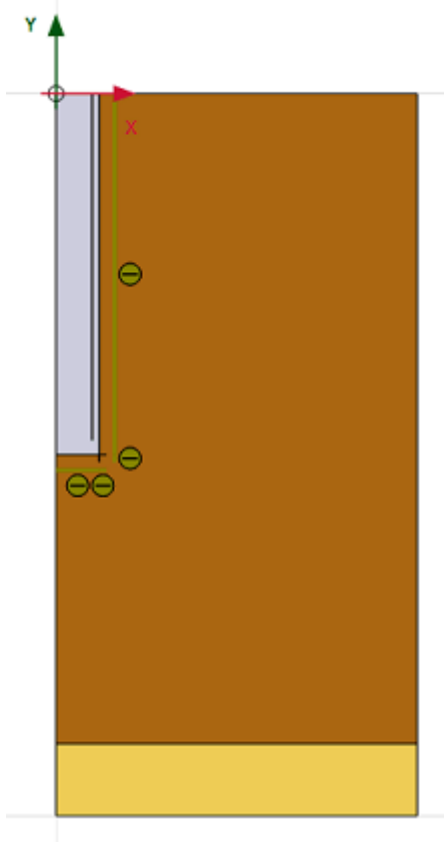


Figure 51. Schematic of the model used in Plaxis

### **6.1.2 Material Characteristics:**

The soil modeled had the same characteristics as that of the clay used in the experiments presented in Section 2.2. Mohr-Coulomb model was used to describe the behavior of the soft clay and sand. The drainage type is Undrained A for the clay and Drained for the sand. The concrete was introduced as a non-porous linear elastic soil cluster with characteristics mentioned in Section 2.1.

## **6.2 Boundary Conditions:**

### ***6.2.1 Mechanical Boundary Conditions:***

The vertical load was applied at the pile head as distributed load. The deformation was restricted horizontally for the vertical boundaries and vertically for the bottom boundary of the model.

### ***6.2.2 Thermal Boundary conditions:***

The thermal boundary conditions were applied as constant temperatures. The room temperature was induced by a thermal flow in the initial phase and as thermal lines at the vertical and horizontal bottom boundaries of the model. The thermal cycles were triggered by adding a thermal boundary line inside the pile with a 20 mm cover similar to the S-loop embedded in the experimental pile.

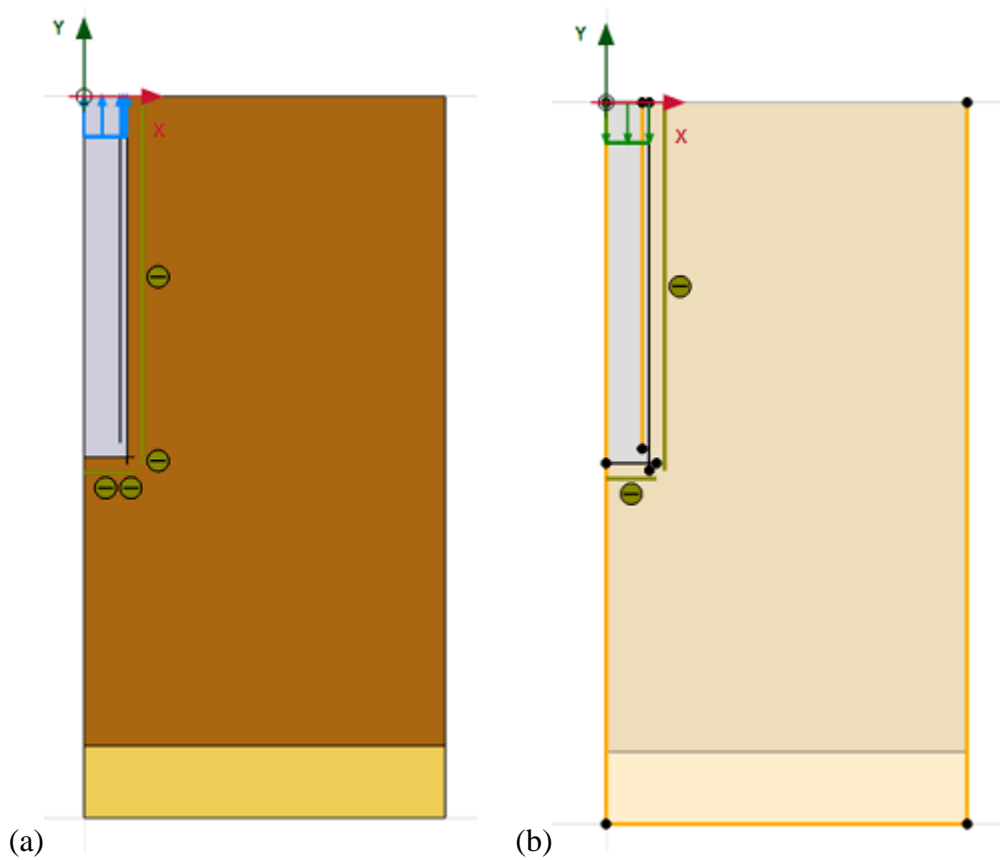


Figure 52. Boundary conditions: (a) mechanical and (b) thermal

### 6.3 Model Analysis

The analysis was done on two stages. The first was to validate the mechanical properties of the soil and pile, while the second to validate the thermal output.

#### 6.3.1 Mechanical Response

This model consisted of three phases: initial, pile installation, and loading the pile to failure. The soil parameters adopted are shown in Table 3. The analysis was done using an elastoplastic calculation.

Table 3. Modeled soil characteristics

Material Characteristic	Soft Clay
Young's Modulus, E (kPa)	4000
Cohesion, $c'$ (kPa)	3
Friction Angle, $\phi'$ ( $^\circ$ )	26
Poisson's Ratio, $\nu'$	0.3

Testing the capacity of the pile was evaluated by applying an upward load of 1.7 kN at the pile head as distributed load in a fast rate over 0.25 Hrs. The results of this phase were compared to the results of the uplift test of the C-Pile in first experiment (Figure 53), since it was not subjected to any thermal cycles or to a sustained load. The results of the numerical analysis of the uplift test shows a good agreement with results of the laboratory test.

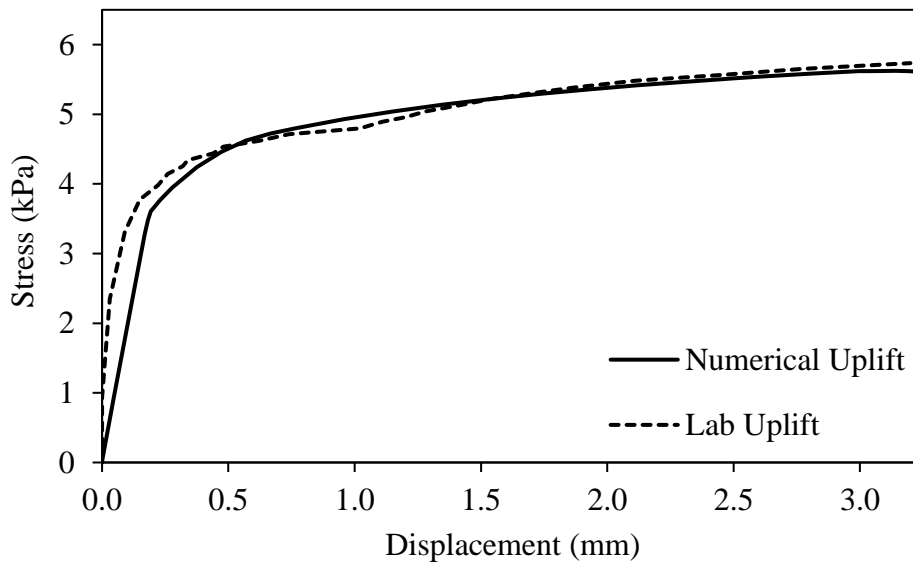


Figure 53. Stress displacement curves

### 6.3.2 Thermal Response

This numerical simulation aimed to verify the thermal characteristics and parameters that were adopted. The used values were taken from performing a thermal test over the soil. Then, a thermal sensitivity was done to best match the thermal response of the energy piles by varying specific heat, thermal conductivity and linear thermal expansion of the soil. The adopted parameters are shown in Table 4. These values fall in the ranges adopted by Gawecka et al. 2017<sup>27</sup> and Laloui et al. 2014<sup>23</sup>.

Table 4. Thermal properties of soft clay

Specific Heat, $C_s$ (kJ/t.°C)	2000
Thermal Conductivity, $\lambda_s$ (kW/m.°C)	$3 \cdot 10^{-3}$
Thermal Expansion, $\alpha$ (1/°C)	$6 \cdot 10^{-6}$

The results presented in Figures 54 and 55, show a coherence in the temperatures reached during heating and cooling with the experimental temperatures. At 80 mm and 400 mm depth, the temperature varies slightly at 360 mm horizontal distance but matches the lab data at small distance from the pile. In addition, taking sections at 80 and 400 mm depth, verify the coherence in reached temperatures at the end of each cycle, at difference distances from the pile surface (Figure 56).

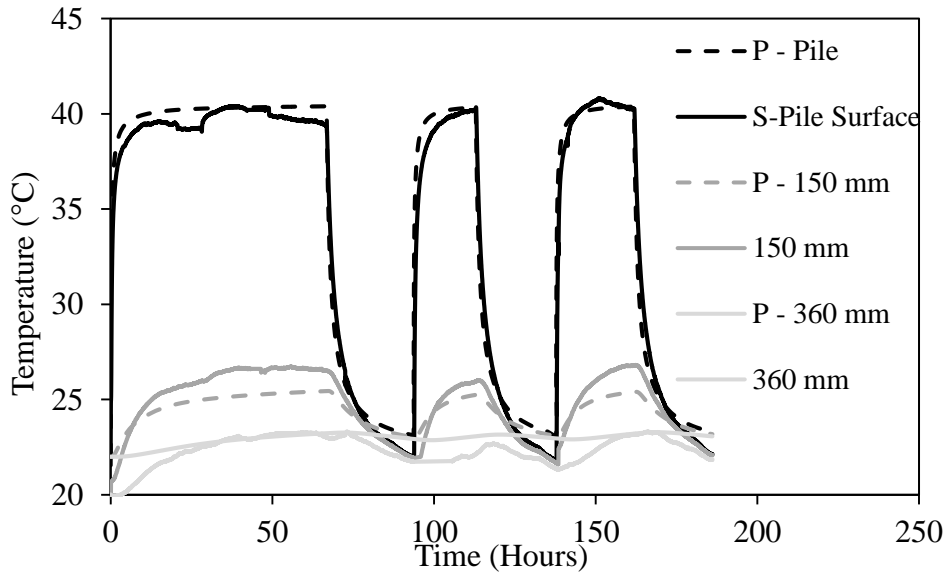


Figure 54. Temperature variation with time during experimental and numerical analysis at 80 mm depth

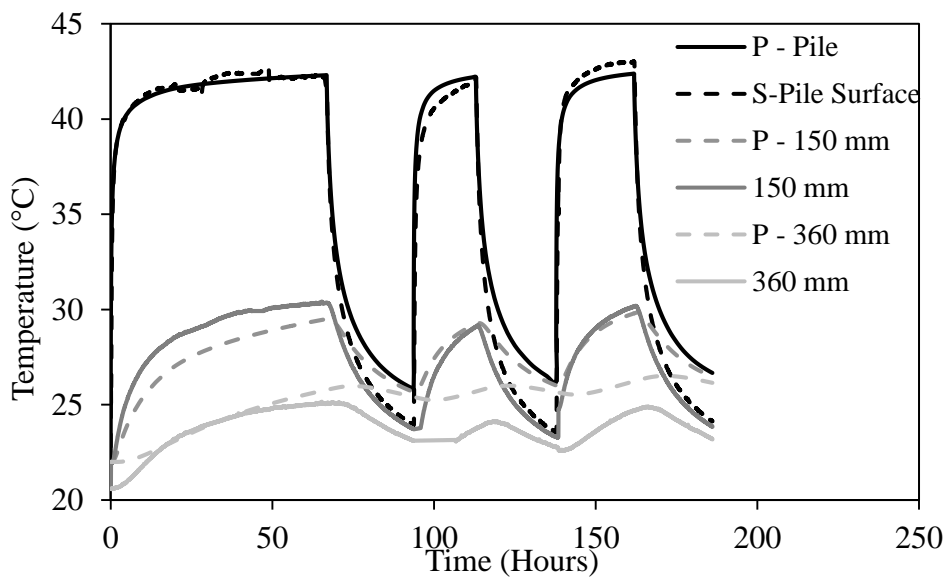


Figure 55. Temperature variation with time during experimental and numerical analysis at 400 mm depth



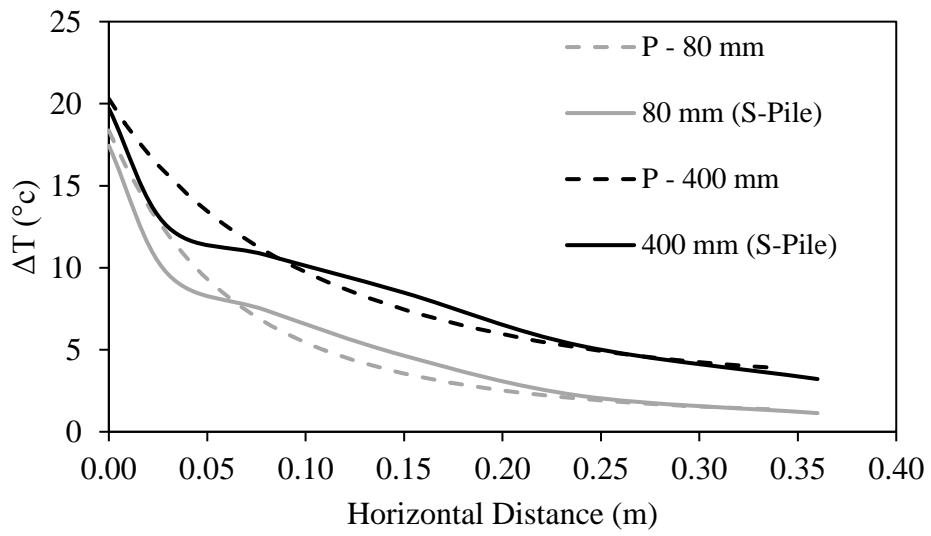


Figure 56. Numerical and experimental (S-Pile) temperature difference (with ambient) variation at horizontal distance



Figure 57. Temperature variation in soil at the end of heating phase in Plaxis 2D

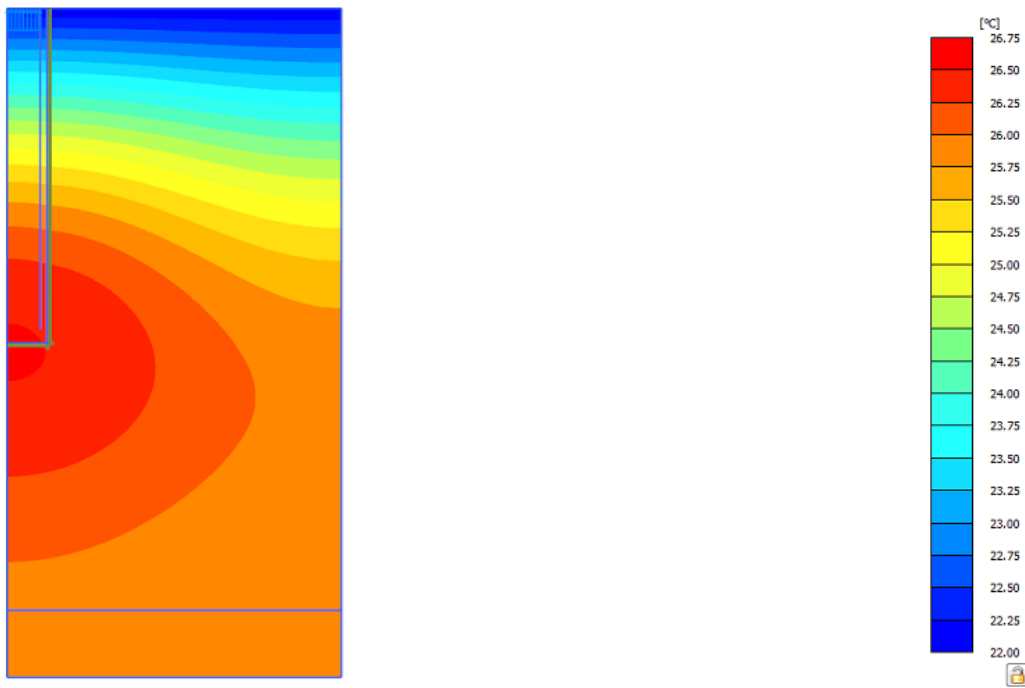


Figure 58. Temperature variation in soil at the end of cooling phase in Plaxis 2D

## CHAPTER VII

### CONCLUSION

The complex thermomechanical processes that occur in energy piles are far from understood. Recent progress in the heat transfer analysis of energy piles provided a good initiation. One critical process is how the expansion and contraction of piles during thermal cycles affect the frictional capacity of the foundation, especially in the long term. This concern may have to be taken into consideration when designing energy friction piles in slightly overconsolidated clays.

Experiment 1 was conducted as a preliminary test to have a better understanding of the general behavior of a geothermal pile. This experiment had two objectives. The first was studying the effect of the thermal cycles on the capacity of the pile, by comparing the energy piles to the control pile. The second is examining the thermal efficiency of different pile configurations, by comparing the S-configuration and the 2U-configuration.

Experiment 2 aimed to study the previously mentioned objectives for E1, but with adding sustained load on the piles. This was possible by comparing the test results of 2U-Pile in both experiments. In addition, the S-Pile was subjected to more cycles to study any variation in the response on the long term. The performance of the S-Pile was compared to that of 2U-Pile of the same experiment.

The results of the first experiment showed a notable decrease in the adhesion between the slightly over consolidated clay and the geothermal piles (~ 20%) and a decrease in the soil-pile interface ductility as a result of the applied heating and cooling cycles. In addition, the pile with the spiral configuration exhibited a higher thermal

efficiency as indicated by the higher heat exchange rate compared to the pile with the 2U-configuration.

Whereas during the second experiment, an irreversible upward pile displacements were generated during thermal cycles with a decreasing rate. This pile head heave is partially due to the thermal expansion/contraction of the pile. The accumulated displacement reached 0.6 mm for the 2U-Pile and 1.5 mm for the S-Pile at the end of the cycles under a sustained service load that is equal to about 30% of the ultimate load. In addition, the thermal capacity of the pile given by a specific tubing configuration affected the magnitude of the pile deformation/creep during thermal cycling. Larger pile displacements were noticed for the pile having a higher heat exchange. This creep increased with the increase in the number of thermal cycles.

The numerical analysis in this research did not go beyond validating the used model using the experimental reached results. However it spots the importance of such tool that can mimic the experimental behavior and gives the opportunity to have duplicates of the experiment by varying multiple parameters in a significant time.

The stability of energy piles relies on the shear strength of soil-structure interfaces, and the thermo-hydro-mechanical processes can have a strong effect on the behavior of interfaces between saturated slightly overconsolidated soils and piles. This is because variation in temperature may lead to water flow in the soil.

The results of this pilot experimental program are limited and should be confirmed in the future with additional tests to provide better understanding of the interface response of energy piles in soft clays.

## REFERENCES

1. Bourne-Webb PJ, Freitas TMB, Assunção RMF. Soil – pile thermal interactions in energy foundations. *Géotechnique*. 2015;66(2):167-171. doi:10.1680/jgeot.15.T.017
2. Brandl H. Energy foundations and other thermo-active ground structures. *Géotechnique*. 2006;56(2):81-122. doi:10.1680/geot.2006.56.2.81
3. Brandl H. Thermo-active ground-source structures for heating and cooling. *Procedia Eng*. 2013;57:9-18. doi:10.1016/j.proeng.2013.04.005
4. Blight GE. Interactions between the atmosphere and the earth. *Géotechnique*. 1997;47(4):715-767.
5. Olgun CG, McCartney JS. Outcomes from international workshop on thermoactive geotechnical systems for near-surface geothermal energy: from research to practice. *DFI J - J Deep Found Inst*. 2014. doi:10.1179/1937525514Y.0000000005
6. Gao, J., Zhang, X., Liu, J., Li, K. S., & Yang J. Thermal performance and ground temperature of vertical pile-foundation heat exchangers. *Appl Therm Eng*. 2008;28:2295-2304.
7. Hamada, Y., Saitoh, H., Nakamura, M., Kubota, H., & Ochifuji K. Field performance of an energy pile system for space heating. *Energy Build*. 2007;39:517-524.
8. Jalaluddin, A., Miyara, A., Tsubaki, K., Inoue, S., & Yoshida K. Experimental study of several types of ground heat exchanger using a steel pile foundation. *Renew Energy*. 2011;36(2):764-771.
9. Luo, J., Zhao, H., Gui, S., Xiang, W., Rohn, J., & Blum P. Thermo-economic analysis of four different types of ground heat exchangers in energy piles. *Appl Therm Eng*. 2016;108:11-19.
10. Fadejev J, Simson R, Kurnitski J, Haghghat F. A review on energy piles design, sizing and modelling. *Energy*. 2017. doi:10.1016/j.energy.2017.01.097
11. Batini N, Rotta Loria AF, Conti P, Testi D, Grassi W, Laloui L. Energy and geotechnical behaviour of energy piles for different design solutions. *Appl Therm Eng*. 2015;122:390-407. doi:10.1016/j.applthermaleng.2015.04.050
12. Cheng-long Wang, BEng Han-long Liu, BEng, PhD Gang-qiang Kong, BEng, PhD Charles Wang Wai Ng, BEng, MSc P. Different types of energy piles with heating–cooling cycles. *Proc Inst Civ Eng - Geotech Eng*. 2017;170(3):220-231. doi:10.1680/jgeen.16.00061

13. Laloui, L., Nuth, M., and Vulliet L. Experimental and Numerical Investigations the Behaviour of a Heat Exchanger Pile. *IJNAMG*. 2006;30:763-781.
14. Bourne-Webb PJ, Amatya B, Soga K, Amis T, Davidson C, Payne P. Energy pile test at Lambeth College, London: geotechnical and thermodynamic aspects of pile response to heat cycles. *Géotechnique*. 2009;59(3):237-248. doi:10.1680/geot.2009.59.3.237
15. McCartney JS, Rossenberg JE. Impact of Heat Exchange on Side Shear in Thermo-Active Foundations. *Proc Geo-Frontiers 2011, ASCE*. 2011:488-498. doi:10.1061/41165(397)51
16. Amatya BLL, Soga K, BOURNE-WEBB PJJ, et al. Thermo-mechanical behaviour of energy piles. *Géotechnique*. 2012;62(6):503-519. doi:10.1680/geot.10.P.116
17. McCartney JS, Murphy KD. Strain Distributions in Full-Scale Energy Foundations (DFI Young Professor Paper Competition 2012). *DFI J - J Deep Found Inst*. 2012;6(2):26-38. doi:10.1179/dfi.2012.008
18. Akrouch, G., Sanchez, M., and Briaud J. Energy Piles for Heating and Cooling Purposes. In: *Proceedings of the 5th International Young Geotechnical* . ; 2013:161-164.
19. Stewart, M. and McCartney JS. Centrifuge Modeling of soil structure interaction in energy foundations. *J Geotech Geoenvironmental Eng*. 2014;140(4).
20. Bourne-Webb P, Burlon S, Javed S, Kürten S, Loveridge F, Bourne-Webb, P., Burlon, S., Javed, S., Kürten, S., and Loveridge F. Analysis and design methods for energy geo structures. *Renew Sustain Energy Rev*. 2016;65:402-419. doi:10.1016/j.rser.2016.06.046
21. Uchaipichat, A., and Khalili N. Experimental investigation of thermo-hydro-mechanical behaviour of an unsaturated silt. *Geotechnique*. 2009;59(4):339-353.
22. Yavari N, Tang AM, Pereira JM, Hassen G. Mechanical behaviour of a small-scale energy pile in saturated clay. *Géotechnique*. 2016;66(11):878-887. doi:10.1680/jgeot.15.T.026
23. Ng CWW, Shi C, Gunawan A, Laloui L. Centrifuge modelling of energy piles subjected to heating and cooling cycles in clay. *Géotechnique Lett*. 2014;4(4):310-316. doi:10.1680/geolett.14.00063
24. Bourne-Webb PJ. An overview of observed thermal and thermo-mechanical response of piled energy foundations. In: *European Geothermal Congress 2013*. ; 2013:1-8.
25. Fuentes R, Pinyol N, Alonso E. Effect of temperature induced excess porewater pressures on the shaft bearing capacity of geothermal piles. *Geomech Energy Environ*. 2016. doi:10.1016/j.gete.2016.10.003

26. Khosravi A, Moradshahi A, McCartney JSJS, Kabiri M. Numerical analysis of energy piles under different boundary conditions and thermal loading cycles. *E3S Web Conf.* 2016;9:2-7. doi:10.1051/e3sconf/20160905005
27. Gawecka MEng KA, G Taborda MEng DM, Potts DM, et al. Numerical modelling of thermo-active piles in London Clay. 2017. doi:10.1680/jgeen.16.00096
28. David M. Potts and Lidija Zdravković. *Finite Element Analysis in Geotechnical Engineering: Volume Two - Application.*; 2001.